

Quantifying physiological responses to physical injury in *Porites lobata*, using a transcriptomic approach

By
Colin Lock

A thesis proposal submitted in partial fulfillment of the
requirements for the degree of

Master of Science
In
Biology

Table of Contents

1. Abstract.....	4
2. Introduction	5
2A. Threats to Guam’s coral reefs.....	5
2B. Guam’s response to these threats.....	6
2C. Coral restoration.....	7
2D. <i>Porites</i> as a study genus	10
2E. Transcriptomics.....	13
3. Research questions.....	18
4. Methodology.....	18
4A. Sampling of source colonies.....	18
4B. <i>Porites</i> DNA barcoding and algal symbiont profiling.....	19
4C. Micro-fragmentation, <i>ex situ</i> rearing, and outplanting	20
4D. Maintenance and Response Metrics.....	21
4E. Transcriptomic lab work.....	22
4G. Differential Gene Analysis and Gene Ontology.....	24
5. Results.....	25
5A. <i>Porites</i> DNA barcoding and Algal symbiont profiling.....	25
5B. Micro-fragment growth analysis	27
5C. Co-expression of distinct gene networks separate developmental phases and stress events.....	29
5D. Pairwise comparisons.....	34
6. Discussion.....	42
6A. Energetic trade-offs.....	44
6B. The general coral stress response.....	45
6C. Calcium homeostasis disruption.....	47
6D. Antioxidant defenses.....	50
6E. Protein turnover.....	52
6F. Impacts of physical injury on the host-symbiont relationship.....	53
7. Conclusion.....	54
8. References.....	56
9. Supplemental information.....	68

List of figures and tables

Figures:

Figure 1	Study location and sample colony	19
Figure 2	A freshly cut micro-frag, outplanting design, and a transplanted micro-frag	21
Figure 3	The timeline of transcriptomic sampling	23
Figure 4	Eight weeks of growth in one of the <i>Porites lobata</i> micro-fragments	26
Figure 5	The average weekly surface for the 42 <i>Porites</i> micro-fragments over the 8-week experiment	28
Figure 6	Heat map of significantly differentially expressed genes identified by spline regression analysis	30
Figure 7	Major patterns of gene expression clusters through the time series with GO enrichment patterns	32
Figure 8	Description of differentially expressed metabolic processes for each transition state	43
Figure 9	Cell diagram of the integration of calcium homeostasis disruption (A), Endoplasmic-Reticulum (ER) stress (B), protein anabolism (D) increased energy production (C), and protein degradation (D) found upregulated 24 hours after physical injury.	45
Supplemental figure 1	Proportion of Symbiodinium Clade by source <i>Porites lobata</i> colony	68
Supplemental figure 2	Maximum Likelihood tree of phylogenetic relatedness based on cytochrome b (mt-20)	69

Tables:

Table 1	The number of differentially expressed genes between all pairwise timepoints for coral host and symbiont	35
Supplemental table 1	The number of raw reads, after quality trim, paired and aligned against reference transcriptome	69
Supplemental table 2	Number of sequences in the reference transcriptome after each filtering step	71
Supplemental table 3	Benchmarking Universal Single-Copy Orthologs (BUSCO) table of transcriptome completeness scores based on metazoan lineage.	72
Supplemental table 4	Table of significantly differentially expressed genes of interest	72

1. Abstract

Coral reefs are space-limited ecosystems under increasing threat from global climate change. Coral restoration may be useful in preserving biological and ecological function by mitigating coral loss and maintaining structural integrity and complexity of the reef. Fragmentation is a successful life history strategy for many corals in response to physical disturbance and is an integral part of coral restoration. Coral species that can rapidly recover from fragmentation are able to survive and actively compete for space. In this study, we utilized RNA-seq technology to understand physiological responses of *Porites lobata* colonies to physical fragmentation and outplanting, which have not been characterized, but are essential processes for coral restoration efforts. Our results demonstrate that *Porites lobata* fragments undergoing physical injury recover through two distinct phases: rapid wound regeneration of the cut margins followed by a slower growth phase that cements the colony to the substrate. Our study found rapid physiological responses to acute physical injury and outplanting in the coral host that involved significantly increased energy production, calcium homeostasis disruption, and ER stress leading to increased antioxidant expression and rates of protein turnover. We hypothesized that phosphoinositide-mediated acute calcium homeostasis disruption stimulates wound recovery processes in response to physical injury. Contrary to other coral transcriptomic experiments, symbiont gene expression revealed extremely low gene differences in response to fragmentation, growth, and outplanting. These results provide insight into the physiological mechanisms that allow for rapid wound recovery and stabilization in response to physical injury in corals, which informs restoration efforts.

2. Introduction

2A. Threats to Guam's coral reefs

Coral reefs are among the most productive ecosystems on the planet and support the livelihoods of millions of people via food security and tourism (Moberg & Folke, 1999). Guam relies heavily on the productivity of its reefs to support tourism, supplement food sources, and provide cultural identity. The total economic value of Guam's reefs is estimated at US\$322.9 million per year, from tourism, coastline protection, and food security (Spalding et al., 2017). To preserve these valuable systems, we must understand the functioning of the major ecosystem engineer, reef coral, and the threats facing it (Moberg & Folke, 1999).

Several human-induced stressors have interacted over the past several decades to drive the decline of Guam's reefs. Tourism and commercial fishing, although economically important for many island nations, have caused reductions in coral cover, fish abundance, and diversity. Using data collected in the Red Sea, researchers determined that approximately 4,000-6,000 divers per year can visit a dive site, above which a significant coral cover loss and physical damage is expected (Hawkins & Roberts, 1993). It has been estimated that 140,000 tourists participate in scuba diving in Guam annually (Guam Visitor's Bureau exit surveys, 2019). Several Guam sites, such as Piti Marine Preserve, exceed this number many times (>18,000 divers per year) (Burdick et al., 2008). Coastal development, inadequate sewage treatment, and poor land management practices leading to upland erosion, have increased the sediment and nutrient load on reef flats, contributing to loss of both species and overall coral cover (Burdick et al., 2008; Redding et al., 2013). Furthermore, tourism has led to further coastal development, stormwater and sewage treatment facilities, which exacerbates the sediment and nutrient load on reef flats. Excess nutrients, sediment, and freshwater have been shown to interfere with a variety

of coral's physiological processes, such as growth (Dodge et al., 1974; Crabbe & Smith, 2005), survival (Nugues & Roberts, 2003; Anthony et al., 2007), gamete production (Wittenberg & Hunte, 1992), settlement and recruitment (Hodgson, 1990), immune function (Vega Thurber et al., 2014) and larval survival (Koop et al., 2001). Guam's small-scale reef fishery catch declined as much as 86% since 1950 due to overfishing as well as loss of coral habitat (Zeller et al., 2007). Periodic crown-of-thorns (the predatory seastar *Acanthaster planci*) outbreaks have also been a major cause of reef decline over at least 5 decades (Burdick et al., 2008; Pratchett et al., 2017). Lastly, while the Marianas Archipelago has not seen extensive impacts from coral bleaching for the past 20 years, the threat has become more pronounced in recent years (Burdick et al., 2008; Reynolds et al., 2014; Raymundo et al., 2017, 2019). The summers of 2013, 2014, 2016, and 2017 brought elevated sea surface temperatures to Guam, resulting in mass bleaching events. An estimated 53% total mortality was observed in staghorn populations alone (Raymundo et al., 2017), and 34-37% reduction in live coral cover was estimated island-wide (Raymundo et al. 2019).

2B. Guam's response to these threats

Due to the mounting threats to reefs, there is an increased need for ecological understanding on both global and local levels and adaptive management actions to preserve critical ecosystems (Carpenter et al., 2008; Edwards, 2008). The severity of these mortality events has spurred resource agencies in Guam to a greater commitment to conservation and management of remaining reefs, and restoration to mitigate the effects of widespread coral loss. NOAA's Coral Reef Conservation Program (CRCP), in conjunction with coral reef managers of Guam, have realigned Guam's Coral Reef Management Priorities to focus conservation and restoration efforts and direct funding options to support these efforts. These place-based local

priorities include reducing sedimentation and pollution, protecting Guam’s coral reef fisheries resources, mitigating pressures from military buildup, reducing harmful impacts of recreational use of coral reefs, and improving management to facilitate resilience, recovery, and now restoration. The Guam Coral Reef Resilience Strategy (GCRRS; Hoot, 2019) is designed to guide the community of Guam into a future marked by climate change, through effective fisheries management, decreased land-based sources of pollution, increased reef response and restoration, sustainable reef recreational use, and human community resilience.

Successful, sustainable coral restoration addresses several of Guam’s Coral Reef Management Priorities. In 2013, a collaborative effort was undertaken by University of Guam (UOG) Marine Laboratory, Underwater World (the local aquarium), and SECoRE International, to establish an ocean coral nursery in the Piti Bomb Holes Marine Preserve, as a facility to culture sexual recruits and fragmented corals for rehabilitation and mitigation. A second nursery has been established in Cocos Lagoon, located in the southern tip of Guam, and local coral restoration techniques have been developed and are being tested. Recent efforts to improve restoration techniques have included refining culture and outplanting approaches (Burns, 2018), determining reproductive seasonality in staghorn *Acropora* sp. (Lapacek, 2017), and understanding the influence of water motion on bleaching resilience (Fifer, 2018).

2C. Coral Restoration

Coral reef decline around the world has become so pronounced that passive conservation strategies and natural recovery alone may be inadequate to preserve their biodiversity and productivity (Goreau & Hilbertz, 2005; Rinkevich, 2005; Forsman et al., 2006). Active restoration has been employed in a variety of terrestrial and aquatic ecosystems (Zedler, 2000; Thorhaug, 2011; Lewis, 2016) but only in the last few decades has this strategy gained

popularity in coral reef ecology. Coral restoration may be useful in preserving biological and ecological function by mitigating coral loss and maintaining structural integrity and complexity of the reef (Kojis & Quinn, 2001; Baums, 2008; Edwards, 2008; Barton et al., 2017). Several studies have reported a variety of factors influencing the success of restoration efforts, such as local species composition (Rinkevich, 1995; Edwards & Clark, 1999; Helen, 2000; Epstein & Bak, 2016), different species recruitment rates (Kojis & Quinn, 2001), substrate type (Helen, 2000; Epstein et al., 2003), and fragment or colony size (Hawkins & Roberts, 1993; Forsman et al., 2006, 2015; Okubo et al., 2007). Coral colony size directly correlates with survivorship and fecundity, and thus is important to consider when designing restoration outplanting activities (Lirman, 2000, 2012; Raymundo & Maypa, 2004; Forsman et al., 2006; Barton et al., 2017). Conservation of coral reefs through preventative management actions is the primary goal, but when ecosystems become acutely degraded (ship groundings, extreme weather events, port dredging, etc.) beyond capabilities of natural recruitment and water quality remains favorable, active restoration may be useful (Edwards & Clark, 1999; Rinkevich, 2005; Edwards & Gomez, 2011; Barton et al., 2017).

“Coral gardening” is one of the most common restoration methods, which generally involves procuring minute fragments or larvae from healthy coral populations or “fragments of opportunity” (fragments that have separated from the parent colony and remain unattached and at risk of mortality), and propagating these to create a workable broodstock (Rinkevich, 2005; Herlan & Lirman, 2008; Edwards & Gomez, 2011; Epstein & Bak, 2016). After these colonies have reached a stable size and show a higher chance of survival (Lirman, 2000; Rinkevich, 2005; Barton et al., 2017), small fragments can be carefully pruned and firmly affixed (out-planted) to degraded reefs, while sustaining the initial broodstock for future outplanting (Epstein & Bak,

2016). Fragmentation is a useful technique for restoring corals that naturally fragment, like *Acroporids* (Lirman, 2000; Highsmith, 2007; Lirman et al., 2010), and for some that do not, such as massive *Porites* (Forsman et al., 2006, 2015; Page et al., 2018). Partial mortality caused by disease, bleaching, or predation can also lead to separation of a coral colony. The micro-fragmentation technique, in particular, is the controlled process of cutting coral into minute pieces usable for minimally invasive restoration and standardized growth, fusion, and stress assays/experiments (Forsman et al., 2006, 2015; Page et al., 2018). Epstein & Bak (2016) found that cutting more than 10% of *Acropora* colonies resulted in significantly higher mortality and reduced fecundity of donor colonies, thus underlining the importance of minimal wild sampling and conservation restoration techniques. Edwards & Gomez, (2011) state that minimum coral size for high restoration success is species and site dependent, but generally larger fragments have higher chance of survival. Thus, micro-fragmentation utilizes small fragment size, which alleviates damage to wild stocks, and a nursery phase to rear corals to a minimum size before outplanting to reduce overall mortality. Micro-fragmentation has been shown to be useful in restoring branching *Acropora* (Herlan & Lirman, 2008; Lirman, 2012) and several massive species (Forsman et al., 2006, 2015; Page et al., 2018) on degraded reefs.

Mortality rate and fecundity are strongly correlated with size in many modular organisms, including corals (Hughes & Jackson, 1980; Huges, 1985; Hughes & Connell, 1987; Soong, 1993). Lirman et al. (2010) observed that 2.5 cm branch tips of *Acropora cervicornis* had similar growth rates to 3.5 cm frags, but 74% higher mortality. This association between mortality and fragment sizes can be explained by a number of factors, such as increased algal competition, disease and predation susceptibility, and lower lipid reserves (Rinkevich, 2005; Okubo et al., 2007; Lirman et al., 2010). In addition to size-specific mortality, fragmentation can

reduce a reproductive colony to a pre-reproductive state (Wallace, 1985; Harrison & Wallace, 1990; Zakai et al., 2000; Okubo et al., 2007). The reduced sexual reproduction of a fragmented coral colony is correlated with fragment size and the developmental stage of the oocytes (Okubo et al., 2007). This indicates that there is a life history tradeoff causing colonies to invest in rapid growth and forgo sexual reproduction until a minimum size is reached. Size and seasonal sexual reproduction should thus be considered when employing fragmentation techniques. This lower survivorship in small fragments (Hughes, 1989; Harrison & Wallace, 1990; Smith & Hughes, 1999; Zakai et al., 2000; Okubo et al., 2005; Rinkevich, 2005; Highsmith, 2007) has been overcome in some studies by rigorously controlling nursery conditions, such as suspending corals off the seafloor to reduce sedimentation and disease, but this is not always achievable for *in situ* nurseries due to local factors and costs (Spurgeon, 2001; Rinkevich, 2005; Forsman et al., 2006; Lirman, 2012). Considering these factors, the microfragmentation technique is a promising, minimally invasive strategy for coral restoration that merits further research (DeSalvo et al., 2010; Forsman et al., 2015; Page et al., 2018)

2D. *Porites* as a study genus

Most coral restoration efforts have, to date, focused on branching corals (Edwards & Clark, 1999) due to their heavily threatened status, fast growth, and ease of propagation. However, in order to preserve diversity and ecosystem function, restoration projects should consider all growth forms that contribute to the structural complexity of a reef. Other coral growth forms, such as stress-resilient, slow-growing massives, are essential to the ecology of the reef (Loya et al., 2001; Herlan & Lirman, 2008; Lirman, 2012; Barton et al., 2017; Page et al., 2018). Massive *Porites* sp., for instance, are a significant contributor to coral reef accretion, can stabilize rubble zones, and form the first stages of a reef in soft sediments (Done & Potts, 1992;

Potts et al., 2007). Due to massive *Porites*' slow growing nature, massive colony morphology, general bleaching resistance, and dense skeleton, it is an ideal candidate for exploring the micro-fragmenting technique. Recent studies have shown low mortality and up to 23 cm² per month of growth in *Porites lobata* undergoing micro-fragmentation (Forsman et al., 2015).

Massive *Porites* spp. are dominant, resilient reef builders found throughout the tropics and exhibit a mix of reproductive modes: some are broadcast spawners, others are brooders (Kojis & Quinn, 1981), and most are gonochoric (single colonies produce only sperm or eggs) while a few are hermaphroditic (single colonies produce both sperm and eggs). Massive *Porites* spp. infrequently reproduce asexually and only after very high energy disturbances (Highsmith, 2007), however they are known to have high tissue regeneration capacity in response to physical injury and disease (Palmer et al., 2011). Understanding how *Porites* spp. respond to environmental stressors can help explain their distribution across a reef ecosystem, how they may respond to culture and restoration, and their future success in rapidly changing environments (Palmer et al., 2008; Darling et al., 2012; Smith et al., 2013; Seneca & Palumbi, 2015). *Porites* spp. can acclimate to highly variable environments, such as places with high nutrient and sediment loads, as well as shallow reef flats exposed to significant thermal stress (Done & Potts, 1992). Massive *Porites* spp. have been shown to be bleaching and, subsequently, white disease-resistant (P. W. Glynn, 1993; Loya et al., 2001; Smith et al., 2013).

Resources available to an organism are usually limited and lead to energetic trade-offs between various physiological functions such as wound healing, growth, and reproduction (Kozłowski & Wiegert, 1986; Ward, 1995; Smith & Hughes, 1999). Regeneration of damaged tissue is a crucial component of survival for colonial organisms and has been used as a proxy for a coral's resilience to stressors. Several early coral studies support a "localized regeneration

hypothesis” that states that energy required for lesion healing is sourced only from adjacent cells (Bak & Yvonne, 1980; Bak, 1983; Meesters et al., 1994). However, colony integration and translocation of resources is one of the greatest advantages of colonial organisms to facilitate more efficient regeneration and overall colony survival (Oren et al., 1997, 2012; Ruesink, 1997). Oren et al. (2012) found 2-3 cm lesions in *Favia fava* healed more effectively in large colonies, and polyps up to 15 cm away had reduced fecundity, indicating that resources for regeneration were translocated further than just the polyps directly bordering the lesion, suggesting that corals are capable of more colony integration than previously thought. Rate of coral tissue regeneration decreases with time and increasing lesion size (Lozada-Misa et al., 2015), occasionally leading to permanent areas of dead, exposed skeleton, which can be colonized by competitors and pose a serious threat to colony integrity (Palumbi & Jackson, 1982; Bak, 1983; Meesters et al., 1994; Ward, 1995; Van Woesik, 1998; Oren et al., 2012). Massive *Porites* spp. are known to have a relatively high regeneration capacity, which may be related to the integration of resources throughout their large colony size (Bak & Yvonne, 1980; Kojis & Quinn, 1981; Done & Potts, 1992; Lough & Barnes, 2000) and their higher antimicrobial properties (Palmer et al., 2008), allowing them to mitigate certain stressful environments. However, Lozada-Misa et al. (2015) found that the slow growth of massive *Porites* also limited their lesion recovery rate compared to branching *Porites*. *Porites* spp. have been shown to heal tissue damage from micro-fragmentation within a few days and begin to calcify over the margin within a week (Forsman et al., 2006, 2015).

Massive *Porites* are dominant species that are important for the ecology of Indo-Pacific reefs. Studies have explored basic restoration techniques with this resilient genus but underlying physiological mechanisms that may allude to their success in restoration efforts and future

survival have not been thoroughly explored. Only in recent years have advances in sequencing technology enabled us to use whole transcriptome responses as a proxy for environmental stress and adaptability in corals.

2E. Transcriptomics

To optimize the success of restoration efforts and mitigate the effects of climate change, the physiology of acclimatization and adaptation must be understood (Baums, 2008; Bay & Palumbi, 2015). Acclimatization of corals has been extensively studied in the context of ocean warming (Edmunds & Gates, 1999, 2008; Jones et al., 2008; Palumbi et al., 2014), ocean acidification (Hoegh-Guldberg et al., 2007; Crook et al., 2013), coral restoration (Herlan & Lirman, 2008; Lirman, 2012; Epstein & Bak, 2016), and global, regional, and local biogeography (Bak & Meesters, 2002; McClanahan et al., 2005; Carilli et al., 2009). Determining a coral's acclimation potential to different stressful events helps to design more robust restoration projects but minute or sublethal physiological differences that are not phenotypically obvious have not been previously considered. Transcriptomics is a tool that can elucidate physiological responses to environmental changes, but has been underutilized in restoration science (Baums, 2008; Barshis et al., 2013; Bay & Palumbi, 2015; Forsman et al., 2015; Seneca & Palumbi, 2015; Fifer, 2018). For example, several studies have shown increased growth rate from micro-fragmenting (Forsman et al., 2015; Barton et al., 2017; Page et al., 2018) but the duration of this effect, and its physiological tradeoffs, have yet to be explored. Forsman et al. (2006) found significant differences between *Porites lobata* genotypes in micro-fragment mortality and growth rates, which they attributed to prior health or acclimation, colony size, and genetic and physiological differences between parent colonies. Genetic factors, such as genotype, population connectivity, and transcriptomic responses can dictate a coral's ability to acclimate to

its environments and to stress events (Rinkevich, 2005; Smith et al., 2007; Vermeij et al., 2007; Baums, 2008). While these factors are considered in terrestrial restoration, they have not been widely investigated in corals. Examining coral responses to micro-fragmentation from a transcriptomic perspective will likely provide additional insight into the physiological responses to fragmentation, which may optimize its use in restoration.

Studying gene expression gives us a reliable snapshot of the metabolic processes that an organism is performing when it is sampled (Johansen et al., 2010; L. K. Bay et al., 2013; Pinzon et al., 2015; Maor-Landaw & Levy, 2016). Gene expression can detect minute changes that may not lead to obvious phenotypic responses and therefore allow a more nuanced understanding of responses to environmental differences (Pavey et al., 2012). Collection of a series of timepoints allows us to find statistically significant gene expression patterns, which can indicate a shift in an organism's physiological response. Further, mRNA sequencing allows rapid, reliable quantification of expressed genes (i.e., the transcriptome) at the time of tissue sampling (Johansen et al., 2010). It must be noted that the correlation between mRNA levels and their respective protein concentration in the cell is variable because current gene expression techniques do not capture post-transcriptional modification (Sealfon & Chu, 2011; Maor-Landaw & Levy, 2016). However, transcriptomics remains a valuable tool for identifying potential biomarkers to examine further via proteomics.

The ability to rapidly modulate the transcription of stress response genes is crucial to surviving variable environments. "Transcriptomic resilience" is an organism's ability to return to pre-stressed gene expression levels (Franssen et al., 2011; Thomas et al., 2019). It informs us of the length of the physiological stress response and is a useful predictor of individual tolerance to stressful events (Franssen et al., 2011; Thomas et al., 2019). When corals are presented with

stressful events, the two common physiological responses are an oxidative stress phase (increased production of reactive oxygen species, calcium homeostasis disruption, and increased transcription regulation), followed by cell death (Maor-Landaw & Levy, 2016). The pathways these responses proceed through are dynamic and vary considerably between species (Barshis et al., 2010; Bellantuono et al., 2012; Kenkel et al., 2013; Maor-Landaw & Levy, 2016; Thomas et al., 2019).

Reactive oxygen species (ROS), such as hydrogen peroxide (H_2O_2) and superoxide radicals (O_2^-), are produced in cellular tissue because of oxidative phosphorylation and other cellular metabolism processes, which can lead to damage of cellular DNA, proteins, and lipids. Large antioxidant enzymes (e.g. superoxide dismutases, albumin, catalases) and non-enzymatic, small-molecule antioxidants (e.g. ascorbic acid, glutathione) eliminate ROS species to mitigate cellular damage. Antioxidant enzymes and ROS are in balance under normal cellular respiration. However, when organisms experience environmental disturbance, ROS can initially overwhelm antioxidant defenses and cause oxidative stress leading to cellular damage (Scandalios, 2002).

A variety of antioxidant enzymes have been identified as significant in the Cnidarian oxidative stress response, including heat-shock proteins (HSPs), superoxide dismutases, catalases, glutathione, ferritin, and redoxin (thioredoxin, peroxiredoxin, etc.) (Császár et al., 2009; Maor-Landaw & Levy, 2016). Heat-shock proteins minimize and prevent damage to proteins, and are upregulated in response to a variety of different stressors in Cnidarians including: heat (DeSalvo et al., 2008; Bellantuono et al., 2012; Barshis et al., 2013; Seneca & Palumbi, 2015; Maor-Landaw & Levy, 2016; Oakley & Davy, 2018), macroalgae competition (Maor-Landaw & Levy, 2016; Aguilar et al., 2019), darkness (DeSalvo et al., 2012), hypo-salinity (Ellison et al., 2017), and UV (Tarrant et al., 2014). Ferritin is a highly conserved iron-

binding protein that controls the amount of available ferrous iron (Fe^{2+}), which is involved in free radical generation (Torti & Torti, 2002; Császár et al., 2009). Ferritin levels in invertebrates are thought to be heavily controlled by transcriptional regulation, making it a potentially useful biomarker, as mRNA levels are likely representative of protein concentration (Torti & Torti, 2002; Császár et al., 2009). The strong correlation between various cnidarian stress events and increased concentrations of antioxidants and protein chaperones (heat shock proteins) indicates these molecules are central to the oxidative stress response and may be useful as biomarkers.

Calcium homeostasis plays a crucial role in the cnidarian oxidative stress response (Maor-Landaw & Levy, 2016; Oakley et al., 2017) and performs a variety of complex physiological functions within a cell, such as signal transduction, protein stabilization and folding, energy production, immune response, intracellular transport, cell cycle regulation (cell differentiation and apoptosis), and biomineralization (Berridge & Irvine, 1989; Bagur & Hajnóczky, 2017). Calmodulin is a calcium-binding protein involved in a variety of signaling cascades and is downregulated in response to heat shock in cnidarians (DeSalvo et al., 2008; DeSalvo et al., 2010). Calumenin is an endoplasmic reticulum resident protein thought to be involved in the unfolded protein response and is upregulated (Oakley et al., 2017) and downregulated (Bellantuono et al., 2012) in response to cnidarian stress events.

The phosphoinositide signaling pathway is a group of transmembrane enzymes that are stimulated by a variety of extracellular molecules, which ultimately lead to physiological changes in cell proliferation, survival, metabolism, cytoskeletal rearrangement, and various stress responses. These changes are often mediated by the release of calcium ions from the endoplasmic reticulum. Phospholipase C and 1-phosphatidylinositol 4,5-bisphosphate phosphodiesterase gamma-1 releases inositol 1,4,5-trisphosphate (IP3) into the cytosol causing

an increase in calcium concentrations via the binding of ligand-gated calcium channels on the endoplasmic reticulum (Berridge & Irvine, 1989; Stefan, 2020). Phospholipase C was found downregulated in response to heat stress (Oakley et al., 2017). Despite its crucial role in a variety of cellular functions, the phosphoinositide signaling pathway has yet to be thoroughly explored in cnidarian gene expression.

In recent years, transcriptome databases have greatly enhanced our understanding of gene expression studies and have been compiled for 22 scleractinian corals, including two relevant to this proposed study (*Porites asteroides*, and *Porites lutea*) (Maor-Landaw & Levy, 2016; Y. Zhang et al., 2019). Research at the UOG Marine Laboratory showed that genes conferring resilience to bleaching were more abundant in Guam's reef-flat staghorn corals growing in high water flow environments compared to those in lower flow environments (Fifer, 2018); this phenomenon has previously been described as gene frontloading (Barshis et al., 2013).

Differential gene expression has been described from corals undergoing, and recovering from, disease (Anderson et al., 2016) and bleaching (Bellantuono et al., 2012; Seneca & Palumbi, 2015; Oakley et al., 2017), but not in response to physical injury. Physical injury to corals is a stressful event that requires a rapid response to seal the wound to prevent infection (Bak, 1983; Van Woesik, 1998; Oren et al., 2012). Fragmentation is a stressful event that few massive *Porites* naturally encounter but yet they have been shown to restore successfully from micro-fragmentation (Forsman et al., 2006, 2015; Page et al., 2018). Using transcriptomics to understand how *Porites* respond to physical injury and transition between physiological states (immediate stress response, recovery, growth, and stability) will inform growth and stress experiments, as well as the use of micro-fragmentation as a restoration tool.

3. Research Questions

Transcriptomic responses to physical injury in corals have yet to be examined. The objectives of this proposed research are to understand how *Porites* spp. and their algal symbiont mitigate the stress of the physical fragmentation and what significant gene expression differences can be correlated with immediate responses to physical injury, and subsequent wound healing, survival, length of recovery, and outplanting stress. Quantifying gene expression differences and monitoring the physical metrics of growth rate, health, and survival will allow me to evaluate the response of massive *Porites* spp. to the micro-fragmentation procedure.

- 1.) What phenotypic changes (growth phases, survival, bleaching, disease, etc.) can be observed in response to physical injury and outplanting in *Porites lobata* corals?
- 2.) What quantifiable physiological shifts can be correlated with phenotypic changes observed in response to physical injury and outplanting?

4. Methodology

4A. Sampling of source colonies

Six *Porites* colonies were sourced from the Luminao reef flat, located on the western coast of Guam (Figure 1). The six colonies ranged in size from 15-25cm in diameter. All colonies were collected intact from ~2 m depth from the same reef flat to minimize potential bias of adaptation to different *in situ* conditions. Sample colonies were at least 20 m apart to minimize the possibility that they are clonal. Whole discrete colonies were taken without fragmenting tissue to minimize stress response before the experiment. Colonies were immediately transported in fresh seawater to the UOG Marine Lab and allowed to acclimate and

recover for four weeks in a raceway tank with fresh flowing seawater, shade cloth, and OW-40 Jebao wavemakers (Zhongshan Jebao Electronic Appliance Co.).



Figure 1: Study location and sample colony A: Guam, the study island, located in the Central Northern Mariana Islands (CNMI). B: Location of Luminao reef, the source of experimental massive *Porites lobata* used in this study. C: One of the six *Porites lobata* colonies used in this study with 17cm scale bar.

4B. Porites DNA barcoding and Algal symbiont profiling

Because *in situ* species-level identification is difficult in massive *Porites*, colonies were taken that have similar gross morphology. An mt-DNA barcoding protocol was employed to delineate samples at the species level. Sample mt-DNA was compared against putative massive *Porites* consensus sequences. DNA was extracted using an Epoch Life Sciences elution column extraction protocol following manufacturer's instructions. Then, the extraction was amplified through PCR using 2 mtDNA markers (mt-20 and mt-16 developed by Dr. Michael Hellberg at Louisiana State University). Gel electrophoresis was used to visually assess the quality of the PCR reaction. Successful PCR products were sent for sequencing at Epoch Life Sciences

(Missouri City, TX). Sequence data from each colony was aligned to putative massive *Porites* sequences in Geneious (Auckland, New Zealand) for loci assembly.

To determine the dominant clade of zooxanthellae associated with each sample, transcriptomic samples from each source colony were mapped against symbiont transcriptomes for the four Symbiodiniaceae genera that associate with Scleractinian corals (*Symbiodinium*, *Breviolum*, *Cladocopium*, *Durusdinium* formerly assigned to clades A, B, C, and D, respectively: LaJeunesse et al., 2018). The number of high-quality (uniqueness) mappings were then used to calculate the relative abundance of each zooxanthellae genera according to Manzello et al., (2019).

4C. Micro-fragmentation, *ex situ* rearing, and outplanting

After four weeks of recovery in the *ex situ* conditions, colonies were cut using a seawater-cooled diamond band saw (C-40, Gryphon Corp. Sylmar, CA, USA) to ~1.5 cm². A total of 36 micro-frags were produced (six per colony), to be destructively sampled for transcriptomics at pre-determined time points. Forty-two micro-frags were produced (seven per colony) to monitor phenotypic response metrics (growth, bleaching, disease, predation, etc.). Micro-frags were created from coral tissue at least 2 cm from the growing edge to reduce variability in growth rates and gene expression differences between fragments. Excess skeleton was removed from the base of each fragment so that micro-frags were relatively the same height. Fragments were attached to ceramic tiles using cyanoacrylate gel and labelled to identify the source colony (Figure 2A). *Porites* are known to produce a good deal of mucus, so they were rinsed with fresh seawater before gluing to assure adhesion.

After the micro-fragments had grown for two months in the tanks, they were outplanted to natural reef substrate in Asan Beach National Park, a protected area on the western coast of

Guam (Figure 2B). They were transported in fresh seawater to the outplanting site and affixed in 3 – 3x4 quadrats (36 total micro-frags) to the reef flat using a splash zone epoxy (Z-spar, Périgny France). Transcriptomic samples were taken to capture the stress of this outplanting event.

3D. Maintenance and Response Metrics

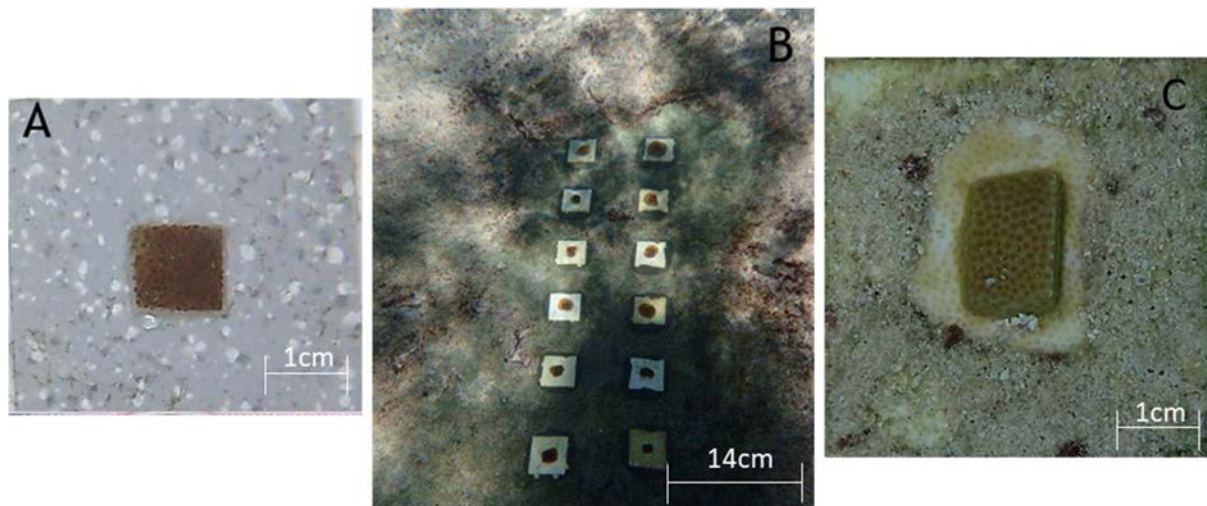


Figure 2: A freshly cut micro-frag, outplanting design, and a transplanted micro-frag. 2A: A photo of a freshly cut *Porites lobata* micro-frag affixed onto a ceramic tile. 2B A photo of the outplants at the Asan beach National Park. 2C: A *Porites lobata* micro-frag showing signs of partial bleaching of the new tissue after outplanting.

Weekly maintenance of the tiles in *ex-situ* culture included removal of algae and detritus from the tiles and tank, and visual inspection of all tiles to remove nudibranch predators. Signs of bleaching, disease, and predation were recorded as well. Water temperature was recorded using a TidbiT[®] v2 Temperature logger (Onset, Bourne, MA, USA) for the duration of the experiment. Weekly photographs of each fragment (Top-down and all 4 sides) were taken using an Olympus TG-5 (Center Valley, PA) in an Olympus underwater housing mounted to PVC stand with a scale bar, CoralWatch pigmentation cards, and estimates of bleaching. Fragment surface area were generated from these collected photos using ImageJ 1.43u[®] (National Institutes of Health, USA).

Pilot studies and micro-fragmentation literature demonstrated that the most rapid growth of *Porites lobata* micro-fragments was immediately following cutting and consisted of rapid wound regeneration over the cut margins. To test for significant differences in growth rate between weeks (difference in surface area from one week to the next) was binned into “growth phases” according to transcriptomic sampling timepoints. From T1 (week 0) to T3 (week 3) were considered phase “A” (Figure 3 and 4) and coincided with rapid wound regeneration over the cut margins of the tile. From T3 (week 2) to T5 (week 8) were considered “B” (Figure 3 and 4) and coincided with a slowing growth rate. A Shapiro-Wilks test was used to assess the normality of the micro-frag growth rates. A repeated measures ANOVA was used to test for significance between these two growth phases, as well as colony and tank replicate differences.

4E. Transcriptomic lab work

Transcriptomic samples were taken at five time points as the corals passed through the fragmentation and outplanting processes: after colony collection and acclimatization but before micro-fragmentation (T1), 24-hr post micro-fragmentation (initial stress phase) (T2), after the first signs of calcification were visible (indicating regeneration) (T3), at 2 months of growth (an estimate of recovery) (T4), and one day after outplanting (a second stress event) (T5) (Figure 2 and 3). T3 was determined after a pilot study indicated that the corals would rapidly seal their cut margins within 2 weeks of micro-fragging.

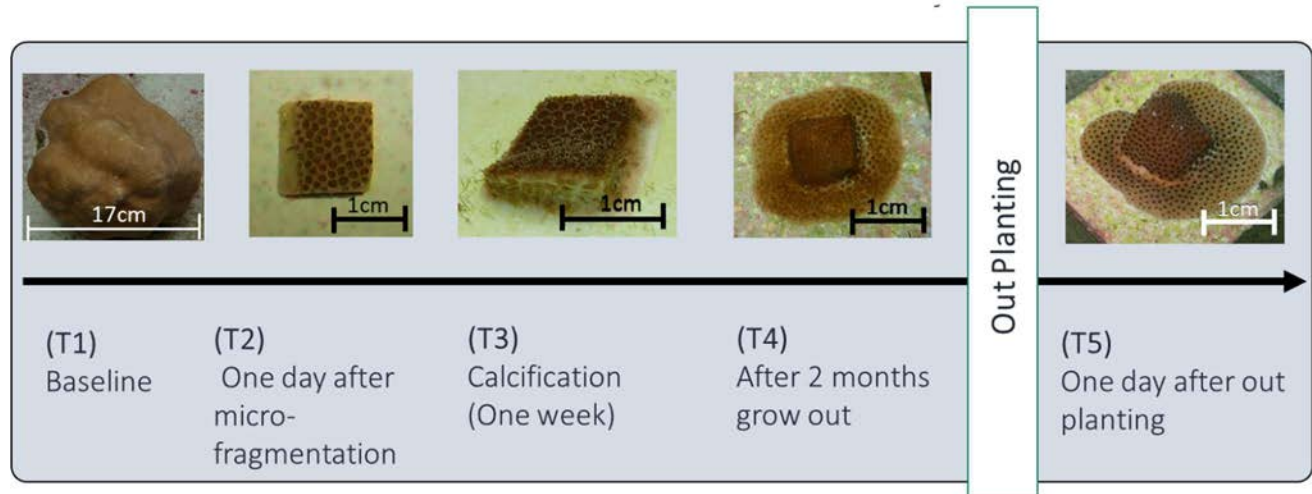


Figure 3: The timeline of transcriptomic sampling.

At each timepoint, one micro-fragment per colony was destructively sampled for RNA extraction. Transcriptomic samples from the tank experiment (T1-T4) were immediately placed into Whirl-Paks© (Nasco, Fort Atkinson, WI), submerged in liquid nitrogen, and stored at -80°C until extraction. Transcriptomic samples from the outplanting experiment (T5) were immediately placed in RNAlater and stored at -80°C until extraction. Total RNA was extracted, using a Qiagen RNeasy kit (Hildenheim, Germany). Extracts were treated with DNase 1 (Invitrogen) to remove DNA, following manufacturer’s protocols. After extraction, total RNA per sample was quantified using a Qubit (Life Technologies, Carlsbad, CA) and qualified using a BioAnalyzer (Agilent Technologies, Santa Clara, CA). Synthesis of cDNA and amplification were performed using the NEBNext® Ultra™ RNA Library Prep Kit for Illumina® (New England Biolabs, Ipswich, MA) following manufacturer’s protocols. The final concentrations of DNA were quantified using Qubit (Life Technologies, Carlsbad, CA). Library sequencing were completed using an Illumina NextSeq 500/550 High Output Kit v2.5 on the Illumina NextSeq 500 (San Diego, CA) located at the University of Guam Marine Laboratory.

Base pairs with a quality score of less than 30 and sequence adapters were trimmed using Trim Galore with Cutadapt (Martin, 2011). All reads were normalized, combined, and renormalized by Trinity's in-silico normalization with max coverage set to 50, before being assembled using the Trinity *de novo* full-length transcriptome reconstruction (Grabherr et al., 2013). After assembly, TransDecoder (Haas et al., 2013) was used to filter sequences by predicting open reading frames and translate the transcriptome to protein sequences. Bacterial genomes from each major clade identified in Schulz et al., (2017) and several fungi, stramenopile, Porifera, Anthropoda, Mollusc, and Annelida genomes were concatenated to form a non-target genome and used in the PERL package Alien Index (Ryan, 2014) to identify and remove potential contaminate sequences from the meta-transcriptome. The filtered reference meta-transcriptome was annotated with gene ontology (GO) terms (Ashburner et al., 2004) by BLAST searching against the combined cnidarian and Zooxanthellae uniprot database with an evaluate cutoff of $1e-5$. The reference meta-transcriptome was then parsed into *Porites lobata* and symbiont transcriptomes. Benchmarking Universal SingleCopy Orthologs (BUSCO) (Simão et al., 2015) was used to determine the completeness of both the *Porites lobata* and symbiont transcriptomes. For the BUSCO analysis, the *Porites lobata* transcriptome was compared against the lineage Metazoa and the symbiont transcriptome was compared against Alveolata with a blast e-value cutoff of $1E-03$. After filtering the *de novo* assembled reference transcriptome, read counts per genes and transcripts per million (TPM) values were generated for each sample using Kallisto (Pimentel et al., 2017).

4G. Differential Gene Analysis and Gene Ontology

The Sleuth package (Pimentel et al., 2017) in R (R Development Core Team, 2018) was used to identify differentially expressed transcripts (q-value < 0.01). Significance of transcripts

mapping to the same gene was then aggregated to the gene level. Time series differential analysis based on natural splines models (likelihood ratio test) was used to discern patterns of expression across the time series, whereas traditional pairwise comparisons (Wald test) was used to identify specific genes and fold changes between timepoints. A natural spline model ($df = 4$) was used to fit “knots” along the observations of the time axis (full model) to determine if expression of a gene follows a pattern significantly better than just noise (null model). A likelihood ratio test between the full and null model within Sleuth was employed to determine significant genes as defined by these 2 models. Genes differentially expressed across the time series were used to generate a transcriptomic heatmap (Figure 6). The gene dendrogram (rows of Figure 6) of the heatmap was cut at height 7.5 (Figure 6) to obtain clusters of likely co-expressed genes. These clusters were visually condensed to form six distinct patterns (Figure 6). Gene ontology (GO) enrichment was performed with REVIGO (Supek et al., 2011) on these patterns (Figure 6).

A Wald test in Sleuth was used to identify gene significance between two specific timepoints. All pairwise comparisons between timepoints were assessed (Figure 3, supplemental Table 4). Since each timepoint depends on the previous state, we focused on the transitions between timepoints (T1vT2, T2vT3, etc.).

5. Results

5A. *Porites* DNA barcoding and Algal symbiont profiling

COX1 and Cytochrome B barcoding of sample corals revealed that 5 colonies (1, 2, 3, 4, & 6) form a monotypic group with known *Porites lobata* sequences (Supplemental Figure 2). Colony 5 was clustered with other *Porites lobata* samples, but distinctly different from the other 5 colonies (Supplemental Figure 2) and based on transcript mapping to the putative

Symbiodiniaceae transcriptomes, the algal symbionts for all samples were primarily (>93%) from the genus *Cladocodium* (Supplemental Figure 1).

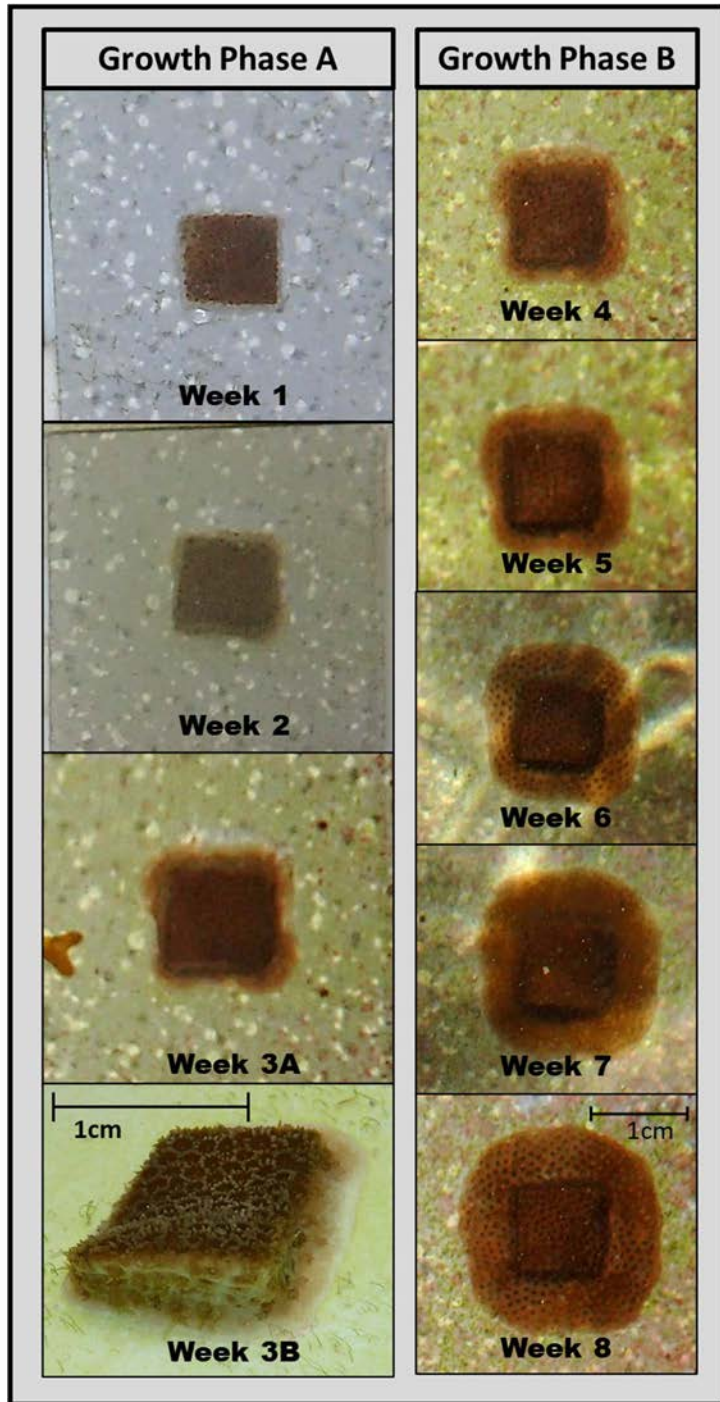


Figure 4: Eight weeks of growth in one of the *Porites lobata* micro-fragments.

Growth phase A (rapid wound regeneration of tissue over cut margins) and growth phase B (slowing of the growth rate as new tissue is deposited onto the tile) are depicted. All photos other than 3B are the same scale with 3B slightly enlarged to show new tissue growth over the cut margins of the fragment.

5B. Micro-fragment growth analysis

All 42 *Porites lobata* micro-fragments survived the experiment and showed no signs of disease, predation, or bleaching until after outplanting. On average, they increased in surface area by 355.4% over the 8-week tank experiment (Figure 4 & 5). The change in growth rate per week was found to be normally distributed (Shapiro-Wilk's test; p-value = 0.0665) and thus able to be assessed for significance with a repeated measures ANOVA. Growth rate between two replicate tanks was not significant (p-value = 0.273). Two distinct growth phases were observed; Growth phase A was associated with the rapid growth of tissue over the cut margins of the micro-frag and phase B was entirely new growth deposited onto the tile (Figure 4). The growth phases A (Week 0-2) and B (Week 3-8) were shown to be significantly different (p-value = 0.000186). Significant variation was also found across the 6 colonies (p-value = 0.002141); Colonies 1-4 continued to grow rapidly after the initial wound recovery (Growth phase A), whereas colonies 5 and 6 growth quickly leveled off after initial wound healing (Figure 5). Interestingly, the new tissue of several micro-fragments (16/32; 50%) showed signs of bleaching during the first two weeks of outplanting, despite growing in similar temperature range as the *ex-situ* tank (figure 2C). No signs of disease or predation were observed during the *ex-situ* culture or after outplanting.

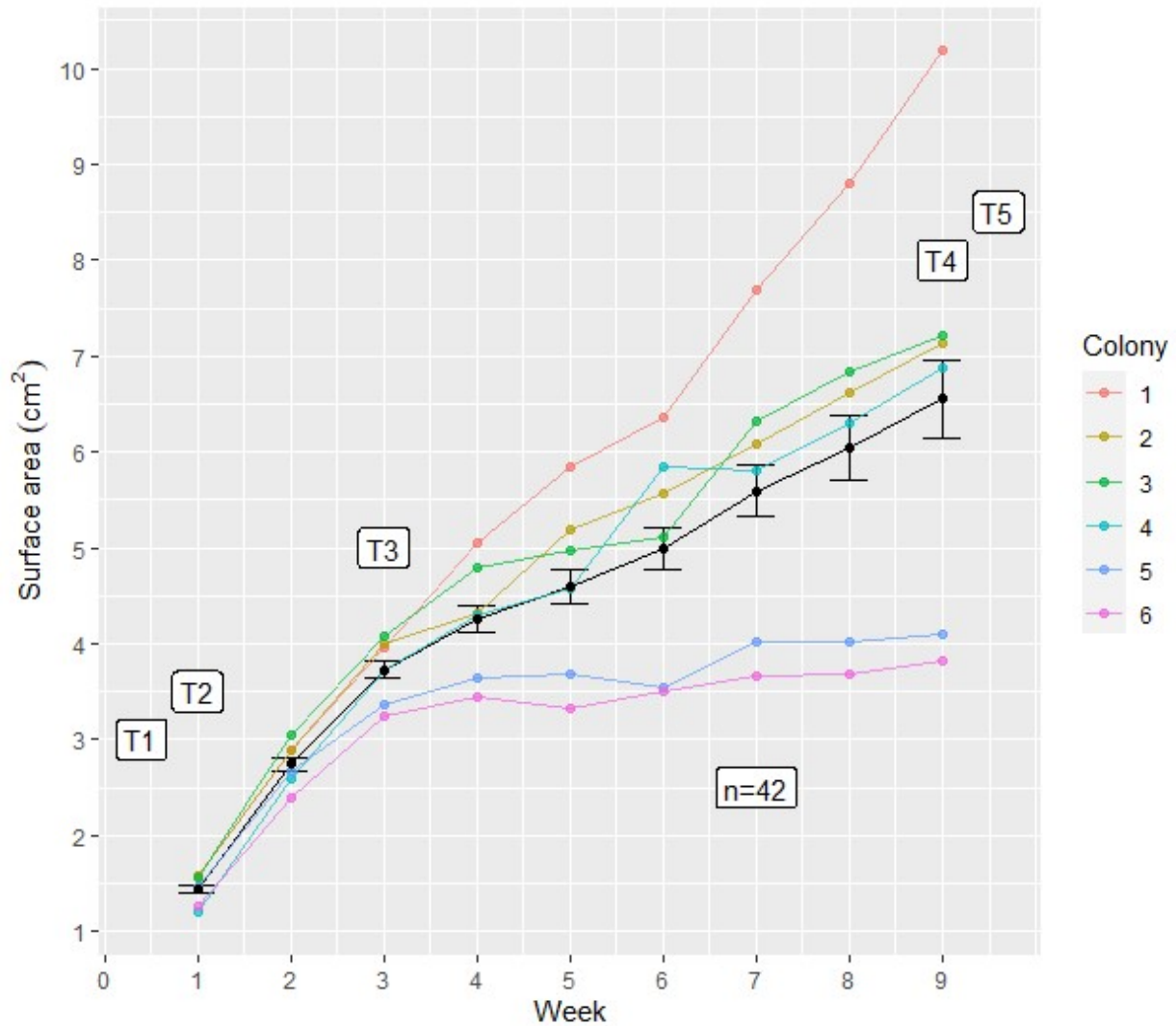


Figure 5: The average (Mean±SE) weekly surface for the 42 *Porites* micro-fragments over the 8-week experiment. T1-T5 represent the transcriptomic sampling points. Colored lines represent individual colony growth, and the black line represents mean micro-frag growth.

5C. Co-expression of distinct gene networks separate developmental phases and stress events.

Sequencing generated between 6.9-54 million reads per sample with an average of 35 million reads per sample (supplemental table 1). Due to low number of reads and separate phylogenetic clustering of colony 5 (Supplemental Figure 1 and 2) this replicate was dropped from further analysis. Trinity de-novo transcriptome assembly generated 1,963,624 coral transcripts, which were filtered and annotated to produce a reference transcriptome comprised of 30,348 coral and 17,994 symbiont genes. For the coral transcriptome, 93.1% of the BUSCO groups had complete gene representation (single-copy or duplicated), while 2.2% were only partially recovered, and 4.7% were missing. For the symbiont transcriptome, 24.6% of the BUSCO groups had complete gene representation (single-copy or duplicated), while 31.0% were only partially recovered, and 44.4% are missing.

A total of 2282 coral genes and 44 symbiont genes were identified as differentially expressed by the spline regression analysis (p -value < 0.01 ; Figure 6). Hierarchical clustering of significantly differentially expressed genes clustered the samples by timepoint replicate and then

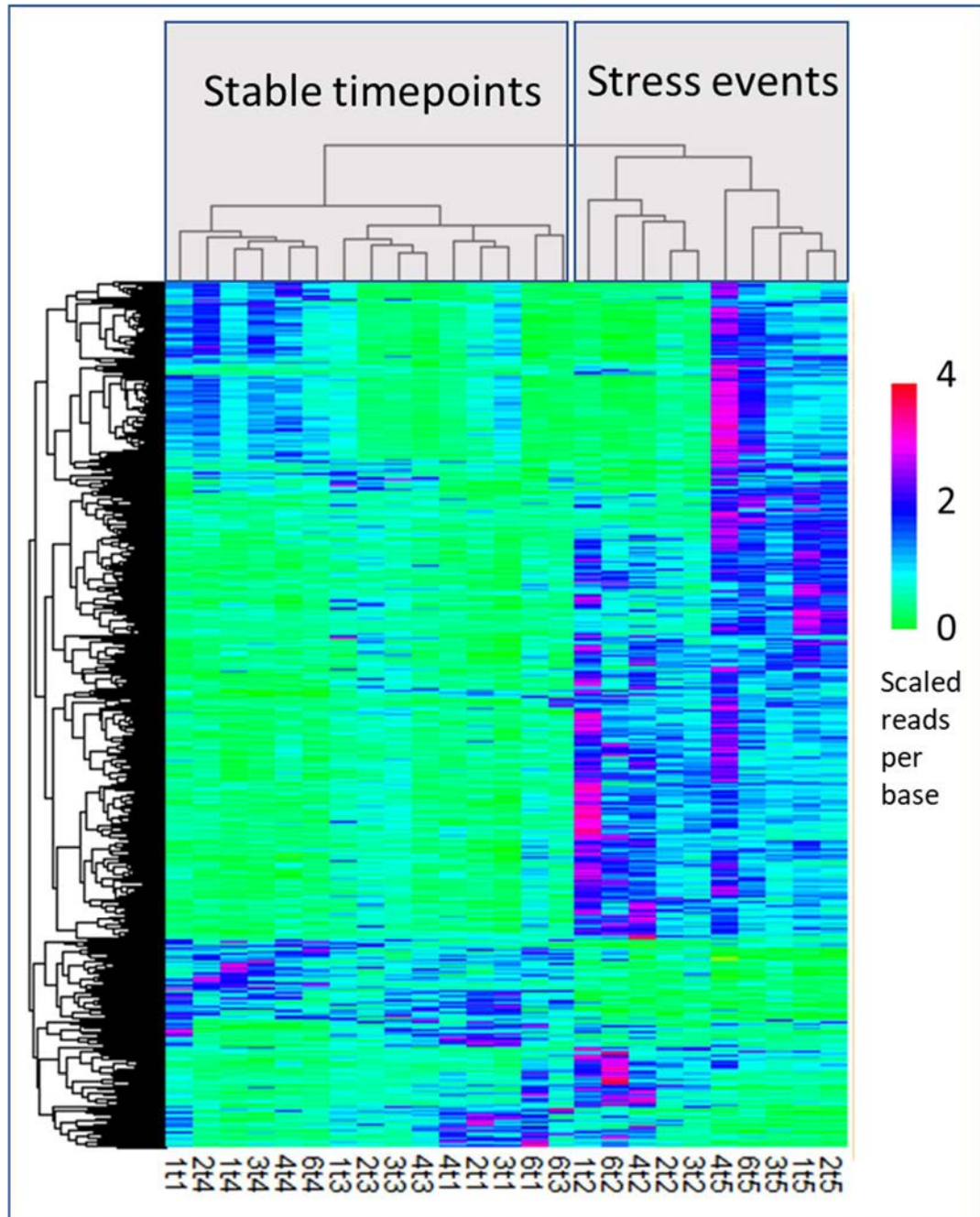


Figure 6: Heat map of significantly differentially expressed genes identified by spline regression analysis. The dendrogram on the left corresponds to clustering of genes (rows) by expression differences across samples (columns). The first number of the column name corresponds to colony replicate and the second refers to the sampling timepoint. The gene expression patterns cluster the samples into two main clusters: the stress events (T2; fragmentation and T5; outplanting) and the more stable growth points (T1, T3, & T5). The color scale corresponds to scaled reads per base of that gene in that sample.

by stress event vs. non-stress event (columns in Figure 6). The dendrogram of genes (rows in Figure 6) produced six major patterns of expression through the time series (Figure 7). Three of these patterns (4-6) consisted of relatively few genes and produced no significant GO enrichment results and were thus removed from Figure 7. The three major patterns consisted of genes that were upregulated at the stress events (T2 & T5, Pattern 1), genes that were downregulated at the stress events (Pattern 2), and genes that were downregulated during growth phase A (when the micro-frags were rapidly growth over their cut margins) (Pattern 3, Figure 7).

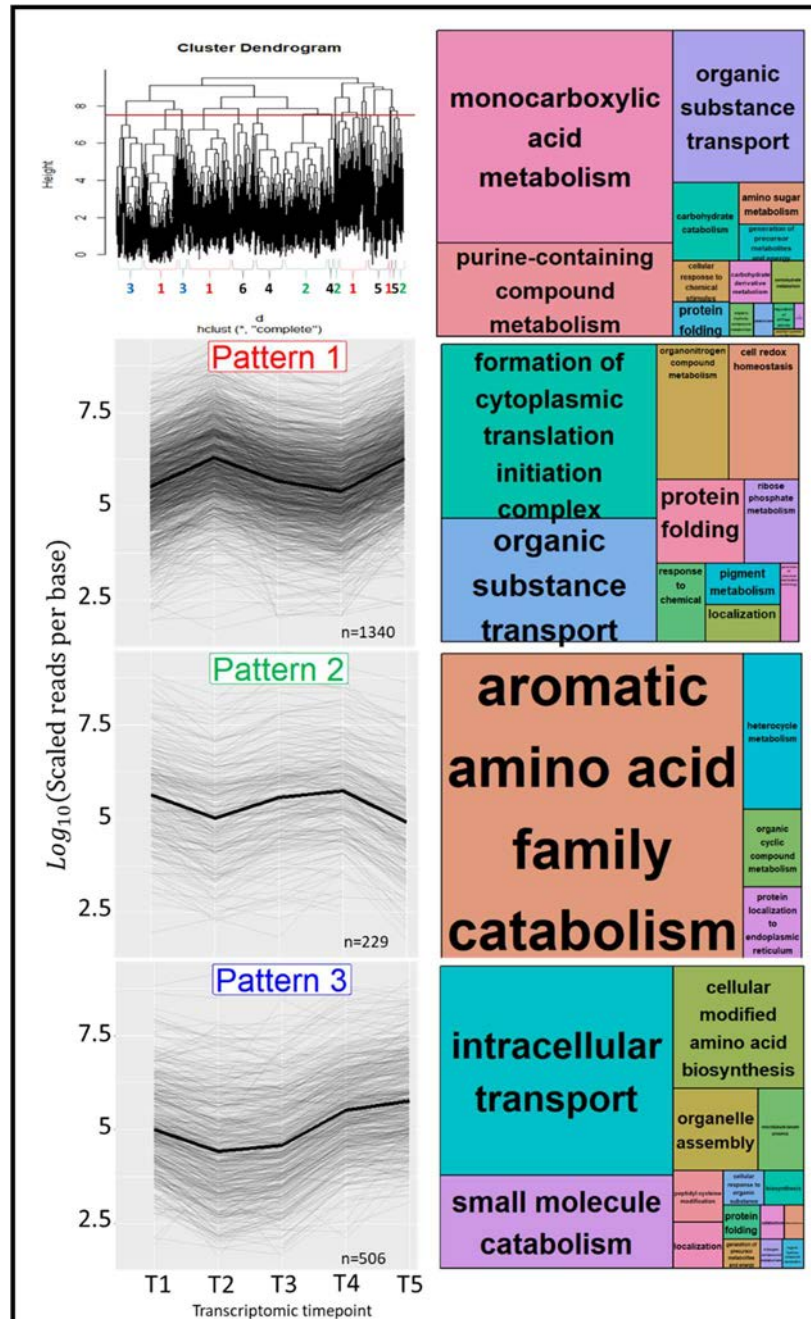


Figure 7: Major patterns of gene expression clusters through the time series with GO enrichment patterns.

Upper left is the cluster dendrogram from the heatmap (Figure 6) with the red line defining the cutting of gene clusters. The upper right figure shows REVIGO GO enrichment treemap of all significant genes (n=2286). The three major gene patterns (pattern 1 = 1340 genes, pattern 2 = 229 genes, pattern 3 = 506 genes) identified through the time series with their corresponding REVIGO GO enrichment treemaps are presented here. Text size correlates with the significance of enriched gene category.

GO enrichment of all identified significant genes (n = 2286) across the time series yielded terms associated with carbohydrate metabolic process (GO:0005975), phosphorus metabolic process (GO:0006793), small molecule metabolic process (GO:0044281), proteolysis (GO:0006508), oxidation-reduction process (GO:0055114), nucleobase-containing compound biosynthetic process (GO:0034654), organophosphate metabolic process (GO:0019637), phosphate-containing compound metabolic process (GO:0006796), phosphorylation (GO:0016310), organic cyclic compound biosynthetic process (GO:1901362), aromatic compound biosynthetic process (GO:0019438), heterocycle biosynthetic process (GO:0018130), ion transport (GO:0006811), organonitrogen compound biosynthetic process (GO:1901566), cellular nitrogen compound biosynthetic process (GO:0044271), transmembrane transport (GO:0055085), organic acid metabolic process (GO:0006082), small molecule biosynthetic process (GO:0044283), carboxylic acid metabolic process (GO:0019752), cellular amino acid metabolic process (GO:0006520), and oxoacid metabolic process (GO:0043436).

GO categories that were significantly upregulated at both of the stress events (Pattern 1, 1340 genes) include formation of cytoplasmic translation initiation complex (GO:0001732), protein folding (GO:0006457), cell redox homeostasis (GO:0045454), generation of precursor metabolites and energy (GO:0006091), ribose phosphate metabolism (GO:0019693), pigment metabolism (GO:0042440), organonitrogen compound metabolism (GO:1901564), response to chemical (GO:0042221), localization (GO:0051179), and organic substance transport (GO:0071702).

GO categories that were significantly downregulated at both stress events (Pattern 2, 229 genes) include aromatic amino acid family catabolism (GO:0009074), heterocycle metabolism

(GO:0046483), organic cyclic compound metabolism (GO:1901360), and protein localization to endoplasmic reticulum (GO:0070972).

GO categories that were significantly downregulated when the micro-frags were recently cut and rapidly growing (Pattern 3, 506 genes) include intracellular transport (GO:0046907), cellular modified amino acid biosynthesis (GO:0042398), small molecule catabolism (GO:0044282), microtubule-based process (GO:0007018), localization (GO:0051179), peptidyl-cysteine modification (GO:0018198), cellular modified amino acid biosynthesis (GO:0042398), protein folding (GO:0006457), catabolism (GO:0009056), generation of precursor metabolites and energy (GO:0006091), organelle assembly (GO:0070925), cellular response to organic substance (GO:0071310), nitrogen compound metabolism (GO:0006807), and organic hydroxy compound metabolism (GO:1901615).

5D. Pairwise comparisons

433 genes were differentially expressed during both fragmentation rapid response and outplanting, whereas 414 and 1190 were unique to fragmentation and outplanting, respectively. Overall, the spline regression analysis yielded broad patterns of enriched gene categories (Figure 6). To obtain finer resolution into the specifics of these gene categories (Figure 6), a traditional pairwise analysis was used (Table 1).

Table 1: The number of differentially expressed genes between all pairwise timepoints for coral host and symbiont.

Coral genes	T1(Baseline)	T2(Immediate response)	T3 (2w of growth)	T4 (2mo of growth)
T1(Baseline)				
T2 (Immediate response)	1648			
T3 (2 weeks of growth)	73	64		
T4 (2 months of growth)	116	1794	2	
T5 (Outplanting)	1753	1207	299	820
<i>Symbiodinium</i> genes				
T1 (Baseline)				
T2 (Immediate response)	7			
T3 (2 weeks of growth)	0	7		
T4 (2 months of growth)	2	42	5	
T5 (Outplanting)	11	210	33	2

For the transition states (T1 vs. T2, T2 vs. T3, etc.), the immediate response to fragmentation yielded the most significant genes (Table 1). Interestingly, the comparison between two weeks (T2) and two months of growth (T3) yielded extremely low differentially expressed genes, potentially indicating a stabilizing of the initial fragmentation stress response after two weeks. Additionally, the comparison between the baseline (T1) and two weeks of growth (T3) yield low differentially expressed genes further indicating a return to stability. The response to fragmentation (T1 vs. T2) yielded twice as many differentially expressed genes as the response to outplanting (T4 vs. T5). Genes previously identified as differentially expressed in cnidarian transcriptomic experiments and other crucial metabolism genes are highlighted in the following section, but a more comprehensive list is provided in Supplemental Table 4.

Oxidative stress

Antioxidant molecules reduce reactive oxygen species, oxidize proteins, and stabilize proteins through cellular stress (Heat shock proteins, components of the thioredoxin system).

Several crucial antioxidant enzymes were upregulated in response to stress in this study (Supplemental Table 4). Thioredoxin, Peroxiredoxin-1, Peptide-methionine (S)-S-oxide reductase (EC 1.8.4.11), and Glutathione transferase (EC 2.5.1.18) were upregulated in response to fragmentation and outplanting. Glutathione peroxidase was upregulated in response to outplanting only. No antioxidant-related genes were found upregulated after two weeks (T3) or two months (T4) of micro-fragment growth. Ferritin (EC 1.16.3.1), an iron-binding protein that controls the amount of available ferrous iron (Fe^{2+}), which is involved in free radical generation, was upregulated after fragmentation and outplanting. Hypoxia up-regulated protein 1 was upregulated after fragmentation and outplanting. Thioredoxin, Glutathione transferase, and Glutathione peroxidase were not identified as differentially expressed after two weeks (T3) and two months (T4) of growth.

Heat shock proteins (HSPs), which serve a variety of protein stabilizing and folding functions in response to stress, were found upregulated in response to immediate fragmentation and outplanting (Supplemental Table 4). HSP70-1 was upregulated after the immediate fragmentation and remained upregulated after two weeks of rapid growth. Four co-chaperones (DnaJ-like proteins) were upregulated in response to fragmentation. Two dnaJ-like proteins were upregulated in response to outplanting. Interestingly, after two weeks (T3) and two months of growth (T4), no HSPs were differentially expressed, indicating a potential return to protein stability. Five out of six HSPs identified be significantly upregulated in response to fragmentation. Six out of seven HSPs be upregulated after the fragments were outplanted.

Protein degradation, synthesis, and transport

Stress events cause a breakdown of normal protein homeostasis leading to increased degradation, synthesis, and transport of proteins (Maor-Landaw & Levy, 2016). A variety of

protein degradation enzymes were identified in response to each stress event (Supplemental Table 4). Ubiquitin-associated ligases, hydrolases, conjugation factors, and transferases were differentially expressed in response to both fragmentation and outplanting. Eight out of twelve and sixteen out of twenty-two ubiquitin-associated proteins were upregulated after fragmentation (T2) and outplanting (T5), respectively, indicating increased rates of protein degradation in response to these stress events. Only one Ubiquitin-associated protein was downregulated at either fourteen days (T3) or two months after fragmentation (T4), which likely demonstrates that the increase in protein degradation processes returns to baseline expression levels quickly following these stress events. Three out of four protein disulfide-isomerases and two 26s proteasome regulatory subunits were upregulated in response to fragmentation (T2).

Several genes associated with protein anabolism were found differentially expressed in response to the stress events, indicating significant increase in protein synthesis. A total of 17 out of 17 translation initiation factors were upregulated in response to fragmentation. Three ribosomal proteins (Ribosome production factor 2 homolog (Ribosome biogenesis protein RPF2 homolog), Ribosomal protein S6 kinase (EC 2.7.11.1), and Ribosomal RNA small subunit methyltransferase NEP) associated with protein biogenesis were upregulated in response to outplanting (T5). In addition, a variety of tRNA ligases, deacylases, synthetases, and hydrolases were all upregulated in response to fragmentation (15/15) and in response to outplanting (5/5). Four out of five aminotransferase enzymes were found upregulated in response to outplanting (T5). 5-aminolevulinate synthase was upregulated in response to fragmentation (T2). Amino acid transporters were found upregulated in response to fragmentation (3/3) and outplanting (1/1).

Cell Cycle

Interestingly, four growth factors and receptors were downregulated in response to fragmentation (T2), when the corals began their most rapid growth phase (Supplemental Table 4; Figure 5). Fibroblast growth factor receptor 1-A was significantly upregulated after two weeks of growth (T3), relative to in response to fragmentation. Important apoptosis-inducing genes (caspase-3, programmed cell death protein 6, and apoptosis regulator BAX) were upregulated in response to both fragmentation (T2) and outplanting (T5). In contrast, Caspase-7 was upregulated only in response to outplanting, whereas bifunctional apoptosis regulator was upregulated after only fragmentation.

Cytoskeleton and extracellular matrix

Cytoskeleton rearrangement is often required to maintain cell motility, structure, and integrity in response to cellular stress. Several cytoskeleton and extracellular matrix genes were differentially expressed in response to the stress events (Supplemental Table 4). Carbonic anhydrase (EC 4.2.1.1), which is understood to be important in coral carbonate deposition (Maor-Landaw & Levy, 2016), and beta-actin was found downregulated whereas three alpha tubulin proteins were upregulated in response to fragmentation (T2). Alpha tubulin was also upregulated in response to outplanting (T5).

DNA damage

Important DNA repair genes were differentially expressed in response to the stress events. DNA topoisomerase 1 (EC 5.6.2.1), which stabilizes the DNA strands while they are unwound for replication, was upregulated in response to fragmentation (T2), whereas DNA double-strand break repair Rad50 ATPase was downregulated. DNA repair proteins (RAD51 homologs) were upregulated in response to outplanting.

Calcium

Calcium acts as an intracellular secondary messenger and mediates a variety of function within the cell. Several genes related to calcium homeostasis disruption were differentially expressed (Supplemental Table 4). Calreticulin, calumenin, Voltage-dependent L-type calcium channel subunit alpha, and Calcium-transporting ATPase (EC 7.2.2.10) were significantly upregulated in response to fragmentation (T2). Calmodulin, which plays an important role in calcification and calcium signaling, was upregulated in response to fragmentation, downregulated after 2 weeks of growth (T3), and not differentially expressed after two months of growth (T4). Calcium and integrin-binding family member 2 was upregulated in response to outplanting. Guanylate cyclase, which is involved in energy conversion, G protein signaling cascade, and is inhibited by high intracellular calcium levels, was downregulated in response to outplanting.

Lipid metabolism

Eleven genes relating to the phosphatidylinositol signaling pathway, which stimulates the release of calcium from the endoplasmic reticulum, were upregulated in response to fragmentation (T2), whereas four out of six were upregulated in response to outplanting (T5). No phosphatidylinositol signaling-related genes were differentially expressed after two weeks or after two months of growth. Sphingolipid 4-desaturase was found upregulated in response to fragmentation and in response to outplanting. Two acyl-coenzyme A thioesterases and Mitochondrial carnitine/acylcarnitine carrier protein CACL, which is involved in lipid catabolism, transport, and signaling, were upregulated, and an O-acyltransferase was found downregulated, in response to fragmentation. Lipid droplet-associated hydrolase, Very-long-

chain 3-oxoacyl-CoA synthase (EC 2.3.1.199), and 3-hydroxyacyl-CoA dehydrogenase type-2 were upregulated in response to outplanting.

Carbohydrate metabolism

A variety of carbohydrate metabolism genes were found upregulated in response to the two stress events. Phosphoglycerate mutase (EC 5.4.2.12), which is involved in glycolysis, was upregulated in response to fragmentation (T2). Phosphoenolpyruvate carboxykinase (EC 4.1.1.32), an enzyme essential for gluconeogenesis, was upregulated in response to fragmentation. Several enzymes involved in the citric acid cycle were upregulated after fragmentation, including ATP-citrate synthase (EC 2.3.3.8), Aconitate hydratase, Mitochondrial pyruvate carrier, and Succinate--CoA ligase (EC 6.2.1.4), and Malate dehydrogenase (EC 1.1.1.37), Mitochondrial pyruvate carrier, and Succinate dehydrogenase (EC 1.3.5.1), in response to outplanting.

Cellular transport

To repair and maintain cellular components during environmental stress, increased transport is often observed. Important genes related to ion, protein, lipid, and carbohydrate transport were differentially expressed (Supplemental Table 4). V-type proton ATPases were upregulated in response to both fragmentation (T2) and outplanting (T5). Zinc, magnesium, molybdate, copper, sodium/potassium transporters, Phospholipid-transporting ATPase (EC 7.6.2.1), and three amino-acid transporters were all upregulated in response to fragmentation. Monocarboxylate transporter 10 was downregulated after two weeks of growth. Zinc, sodium/potassium, Mitochondrial coenzyme A, and Monocarboxylate 10 transporters were upregulated in response to outplanting.

RNA/DNA

Nine out of twelve RNA helicases (EC 3.6.4.13) were upregulated in response to fragmentation (T2). One DNA helicase, RNA-directed RNA polymerase, and four RNA-directed DNA polymerase (EC 2.7.7.49) were downregulated in response to outplanting (T5).

Cellular energy

Responding to environmental stress is an energetically costly processes that must be met with increased energy production for an organism to persist. A total of 36 crucial metabolism genes involved in the electron transport chain and oxidative phosphorylation were differentially expressed in response to fragmentation (T2) or outplanting (T5), indicating significant energy generation in response to the stress events. (Supplemental Table 4). ATP synthase subunits alpha, beta, B1, and gamma were upregulated in response to fragmentation. Adenylate kinase (EC 2.7.4.3), essential to cellular energy homeostasis by converting between various adenosine phosphates (ATP, ADP, AMP), was upregulated in response to fragmentation. Ten subcomplexes of NADH dehydrogenase, five subcomplexes of cytochrome c oxidase, two subcomplexes of Cytochrome b-245, three subcomplexes of cytochrome b-c1, cytochrome b5 and NADPH cytochrome p450 reductase were all upregulated in response to fragmentation, indicating significant energy generation. Two subunits of cytochrome p450 were the only cytochromes that were downregulated in response to the two stress events. Cytochrome b-561 and ATP synthase subunit alpha were the only parts of the electron transport chain upregulated in response to outplanting.

Other

I found a variety of histone-related proteins, which help maintain DNA architecture and assist in replication, repair, and transcription, that were differentially expressed in response to

fragmentation (T2). Histone deacetylase, histone-binding proteins, histone-lysine N-methyltransferase PRDM6, Histone acetyltransferase (EC 2.3.1.48), Histone chaperone asf1, and [Histone H3]-trimethyl-L-lysine (4) demethylase (EC 1.14.11.67) were upregulated in response to fragmentation. Interestingly, two genes involved in the innate immune system were strongly downregulated in response to fragmentation.

6. Discussion

Space on coral reefs is limited and coral species that can rapidly recover from physical disturbances will most efficiently compete for space. Asexual reproduction through fragmentation is a successful life history strategy for many species, but physical wounds can threaten colony integrity if tissue recovery is too slow. Regrowing tissue over damage margins of the coral to prevent infection and stabilizing the colony by depositing new tissue onto the substrate are crucial to colony survival. The physiological responses to physical fragmentation in corals has yet to be explored. Examining gene expression can provide insight into the metabolic processes that dictate survival and initiate rapid wound healing of corals following physical injury. Here, we demonstrate the use of RNA-seq technology to better understand these underlying physiological responses of corals to physical injury. Our results demonstrate that *Porites lobata* fragments undergoing physical injury recover through two distinct phases; rapid wound regeneration of the cut margins and a slower growth phase consisting of stabilizing the colony new tissue deposited onto a substrate. During the rapid growth phase, genes associated with phosphoinositide-mediated acute calcium homeostasis disruption, energy production, antioxidant defenses, and protein turnover were upregulated (Figure 8).

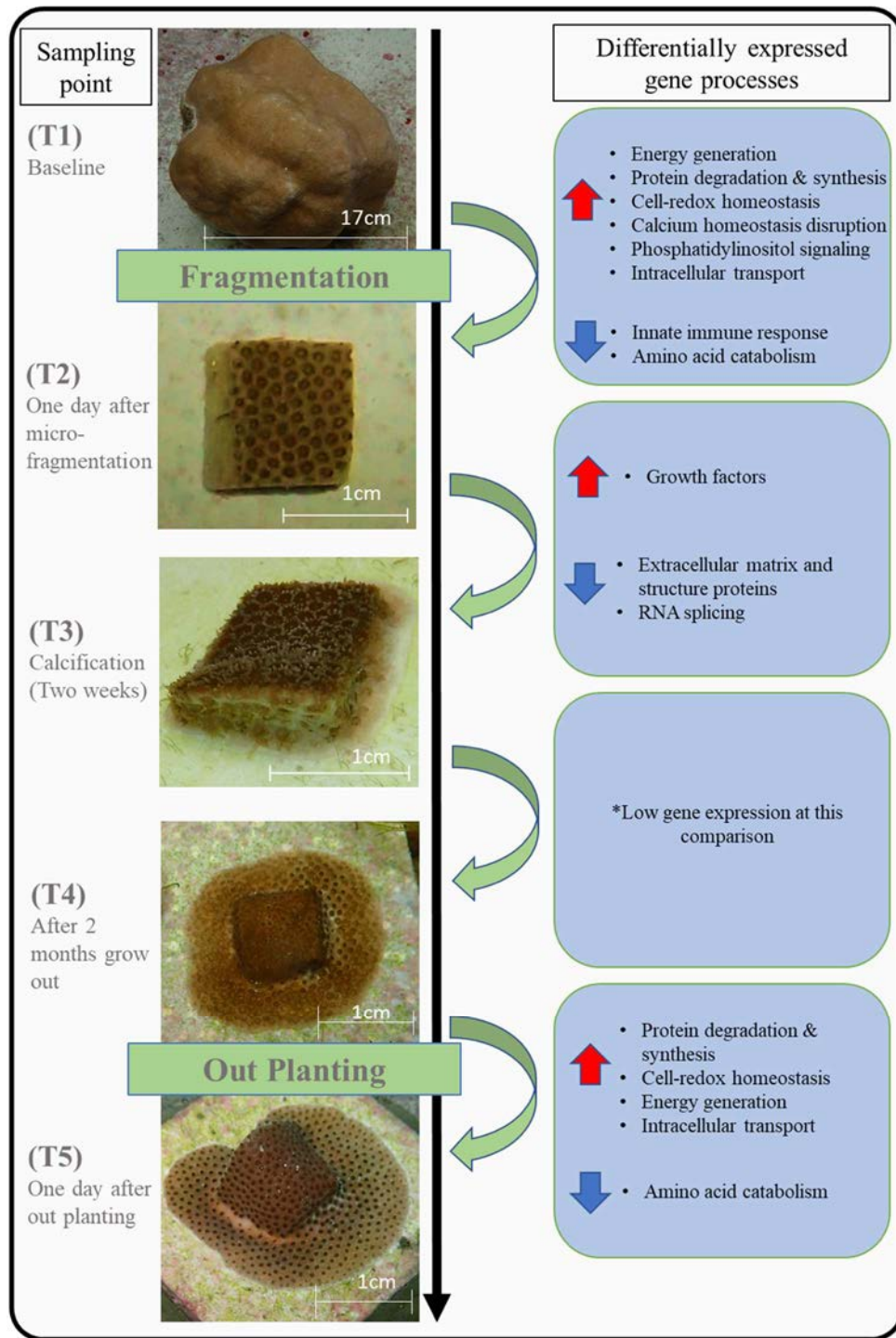


Figure 8: Description of differentially expressed metabolic processes for each transition state.

The photos represent the *Porites lobata* micro-fragment at each transcriptomic sampling point. The red and blue arrows represent general cellular process that are either up- or down-regulated at each transition state, respectively.

Gene processes are based on the pairwise comparisons described in results.

6A. Energetic trade offs

Organisms undergoing stress events have limited energetic resources, which triggers energetic trade-offs between various physiological functions such as wound healing, growth, and reproduction (Kozłowski & Wiegert, 1986; Ward, 1995; Smith & Hughes, 1999). Coral calcification rates are negatively correlated with coral size (Chadwick-Furman et al., 2000) and are increased in response to fragmentation (Lirman et al., 2010; Forsman et al., 2015). In contrast, coral colony size directly correlates with both survivorship and fecundity. Thus, size is crucial to consider when designing restoration outplanting activities (Lirman, 2000, 2012; Raymundo & Maypa, 2004; Forsman et al., 2006; Barton et al., 2017). For example, minimizing this size-specific mortality while stimulating growth rate can be achieved by including a phase to protect small, rapidly growing fragments until a size refuge is reached and outplanting can take place (Rinkevich, 2005). Rapidly regenerating damaged tissue minimizes risk for subsequent infection and is essential for survival of corals undergoing physical injury. In this experiment, two significantly different growth phases were observed. The initial growth phase of *Porites lobata* micro-fragments was characterized by rapid growth for 2wk following fragmentation (Figure 5) and was associated with tissue regeneration over the cut margins (Figures 4 and 5). This initial fragmentation response involved the largest number of genes observed in the experiment and around twice as many as outplanting (Table 1). This response has been reported in coral restoration literature (Forsman et al., 2006; Lirman et al., 2010). The significant variation in colony growth rates following this common, initial growth phase (Figure 5) stresses the importance of understanding intraspecific differences that may influence the success of restoration activities and stress experiments. The following 6 wk of growth was marked by a slowing of the growth rate, albeit with significant colony variation (Figure 5). Very little change

in gene expression was observed between 2 wk and 2 mo of growth (2 genes; Table 1), indicating that once cut margins are sealed and growth rate slows it may be appropriate to outplant the fragments. This point is underlined by the fact that much of the newly grown tissue experienced bleaching within a few weeks of outplanting (Figure 2C).

6B. The general coral stress response

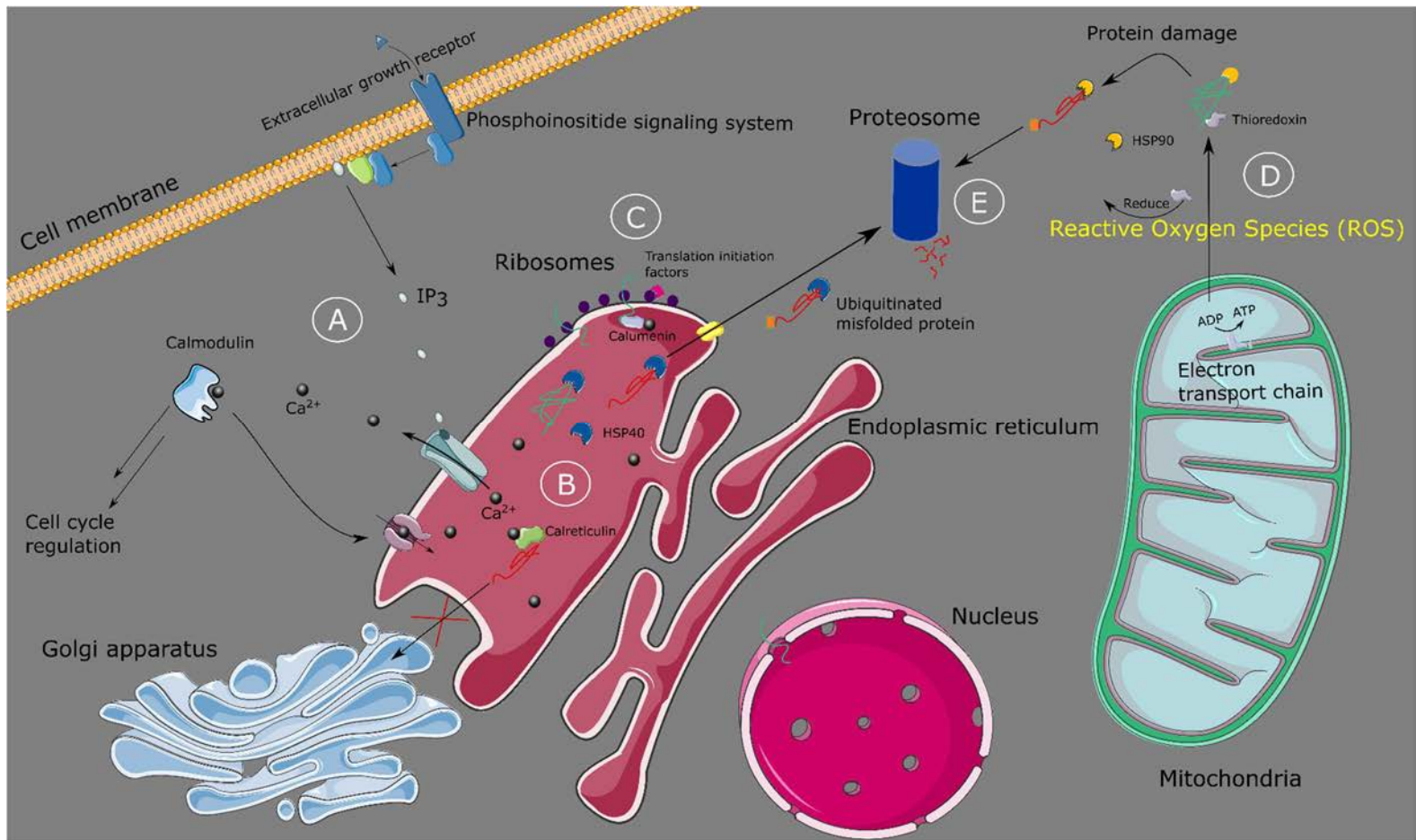


Figure 9: Cell diagram of the integration of calcium homeostasis disruption (A), Endoplasmic-Reticulum (ER) stress (B), protein anabolism (D) increased energy production (C), and protein degradation (D) found upregulated 24 hours after physical injury. 9A: Phosphoinositide signaling releases the secondary intracellular messenger, inositol (1,4,5) trisphosphate (IP3), which binds to ligand-gated calcium ion channels of the ER causing the release of calcium into the cytosol. Calcium disruption is sensed by a variety of molecules including calmodulin

(upregulated in this study), which lead to enzymatic activation and ultimately, cell cycle regulation. Calmodulin also stimulates the reuptake of Ca^{2+} into the ER to prevent prolonged calcium homeostasis disruption and cell death. 9B: Calcium disruption within the ER leads to the Unfolded Protein Response (UPR). Resident proteins upregulated in this study, such as calreticulin, calumenin, and Heat Shock Proteins (HSPs), assist in the folding of proteins and degradation of terminally misfolded proteins. Calreticulin prevents the export of misfolded proteins to the golgi apparatus. 9C: Ribosomal proteins, translation initiation factors, and tRNA enzymes were significantly upregulated and rapidly produce new proteins in response to fragmentation. 9D: To meet energetic demands of the cell under stress, expression of electron transport chain proteins increased. Increased oxidative phosphorylation causes Reactive Oxygen Species (ROS) to leak from the mitochondria causing cellular damage to lipids, DNA, and proteins. Antioxidant molecules upregulated in this study (thioredoxin, glutathione transferase, peroxiredoxin, ferritin) scavenge ROS and assist in protein refolding. Cytosolic HSPs refold damaged proteins and assist in their degradation if they are terminally misfolded. 9E. Terminally misfolded proteins are chaperoned to the proteasome by HSPs after they are tagged for destruction by Ubiquitin-conjugating enzymes. The Ubiquitin/Proteasome system integrate with other signal transduction molecules to regulate cell cycle. Amino acid transporters shuttle degraded polypeptides to ribosomes for protein anabolism

When organisms are presented with environmental stress, the balance between ROS and antioxidant defenses is disrupted, often leading to an increase in antioxidant compounds to prevent significant cellular damage to lipids, proteins, and DNA and, ultimately, apoptosis (Gorman et al., 1999; Scandalios, 2002). Both our spline regression analysis (Figure 6 and 7) and pairwise comparisons provided significant evidence of increased cellular energy generation (oxidative phosphorylation, electron transport chain cytochromes, glycolysis, and citric acid cycle enzymes) in response to fragmentation. These processes likely provide the resources necessary for rapid growth rates, antioxidant defenses, and cellular protein maintenance (Figures 8). Many of the metabolic pathways identified as differentially expressed in this study (Unfolded protein response, HSPs, cell-redox homeostasis, cytoskeleton rearrangement, and calcium homeostasis disruption) coincide with the generalized oxidative stress response described for

cnidarians regardless of the type of stress (Veal et al., 2002; Császár et al., 2009; Tarrant et al., 2014; Maor-Landaw & Levy, 2016; Aguilar et al., 2019). However, fragmentation of *Porites lobata* seems to elicit some unique responses.

Maor-Landaw & Levy, (2016) reviewed 20 years of cnidarian gene expression research and concluded that oxidative phosphorylation-related processes were down-regulated in response to environmental stress. This review also reported that up-regulation of the proteins related to the Unfolded Protein Response (UPR), citric acid cycle, and glycolysis enzymes were unique to branching coral without further clarification. Our study found upregulation of all these pathways in response to fragmentation in *Porites lobata*, a massive coral. Carbonic anhydrases, which catalyzes the hydration of CO_2 to HCO_3^- allowing for easier calcium deposition by the coral, was downregulated in response to heat stress (DeSalvo et al., 2012) and has been suggested to be positively correlated with coral calcification rates (Bertucci et al., 2011). We find down-regulation of 2 carbonic anhydrases, but interestingly this occurred 1d after fragmentation, when the corals begin the most rapid growth phase (Figure 4). This means that although carbonic anhydrases facilitate calcification, they are not the rate limiting step during fragmentation in this study.

6C. Calcium homeostasis disruption

Calcium signaling pathways are ubiquitous signal transduction systems, which regulate a broad variety of cellular processes, such as metabolism, apoptosis, cell proliferation, cell to cell communication, gene expression, and secretion (Stefan, 2020). They are a characteristic state of the cnidarian oxidative stress response (Desalvo et al., 2008; Maor-Landaw & Levy, 2016). Many cnidarian stress experiments report calcium homeostasis disruption, but few have elaborated on the specific signaling mechanisms causing this (Pinzón et al., 2015; Oakley et al.,

2017; Aguilar et al., 2019). Phosphoinositide signaling networks are composed of a series of transmembrane G-coupled proteins that regulate diverse functions in the cell, including the release of Ca^{2+} from the endoplasmic reticulum (ER) via the binding of Inositol (1,4,5) trisphosphate ($\text{Ins}(1,4,5)\text{P}_3$) to ligand-gated ion channel receptors on the membrane of the ER (Berridge & Irvine, 1989; Stefan, 2020). Although it is well characterized in other organisms, the specific roles of phosphoinositide signaling in cnidarians remained uncharacterized and the differential expression of these complexes have been sparsely reported (Oakley et al., 2017; Aguilar et al., 2019). Phosphoinositide phospholipase C, a crucial enzyme that catalyzes the release of $\text{Ins}(1,4,5)\text{P}_3$, was downregulated in response to thermal stress in *Aiptasia* sp (Oakley et al., 2017). This study found significant evidence of upregulation of components of the phosphoinositide signaling pathway (Supplemental Table 4), including Phosphoinositide phospholipase C in response to fragmentation. Several receptors known to stimulate Phosphoinositide signaling were also upregulated, such as tyrosine kinase growth factor receptors, which likely cause the release of the secondary messenger, Ca^{2+} .

While initial calcium homeostasis disruption can stimulate survival pathways, sustained levels of calcium in the cytosol lead to cell death (Orrenius et al., 2003; Bagur & Hajnóczky, 2017). Voltage-dependent and ATPase calcium pumps maintain cytosolic Ca^{2+} levels by sequestering calcium in the ER or secreting it extracellularly, which were upregulated in response to fragmentation and at the same time as calcium homeostasis disruption genes (Supplemental Table 4). This suggests that calcium concentrations are being acutely disrupted likely leading to initiate of survival pathways that promote rapid wound regeneration. Although we do not find upregulation of mitochondrial calcium transporters, increasing concentrations of mitochondrial Ca^{2+} have been shown to stimulate certain energy generating dehydrogenases

(pyruvate dehydrogenase, alpha-ketoglutarate dehydrogenase) and ATP synthase (Tarasov et al., 2012; Bagur & Hajnóczky, 2017), which corroborates with increased energy generation observed in response to fragmentation. The concurrent upregulation of calcium-releasing mechanisms (phosphoinositide signaling) and calcium-dependent ATPase pumps (Supplemental Table 4) immediately following fragmentation when we observe the beginning of rapid growth (Figure 5) suggest that calcium homeostasis is acutely disrupted by physical injury, potentially leading to stimulated cell proliferation and wound regeneration, but quickly removed from the cytosol to prevent cell death and promote recovery.

Ca^{2+} increases in the cytosol are sensed by various Ca^{2+} -binding proteins, including some differently expressed in this study: calmodulin (CaM), calreticulin, and calumenin (Supplemental Table 4). These Ca^{2+} -binding proteins initiate signaling cascades that ultimately lead to shifts in the organism's metabolism. Calmodulin are ubiquitous, calcium-binding proteins that regulates a broad variety of cellular functions, such as cell cycle, in response to calcium homeostasis disruption (Bagur & Hajnóczky, 2017; Huang et al., 2018). Contrary to findings of other cnidarian stress experiments (Desalvo et al., 2008; Aguilar et al., 2019), CaM was upregulated in response to fragmentation and then downregulated after two weeks of rapid growth. This potentially indicates a return to basal intracellular calcium levels and stability. Interestingly, CaM proteins have been identified as regulators of settlement and metamorphosis in *Acropora millepora* (Reyes-Bermudez et al., 2012, 2016) and may be responsible for interpreting the initial calcium homeostasis disruption leading to rapid wound regeneration in response to physical injury in this study. Calreticulin and calumenin are both ER resident proteins, which along with HSP-40s (Dnaj proteins), prevent the export of misfolded proteins that accumulate during oxidative stress, and were upregulated in response to fragmentation. Calumenin has been

implicated in host-symbiont recognition (Ganot et al., 2011) and is both downregulated in *Acropora millepora* (Bellantuono et al., 2012) and upregulated in *Aiptasia* sp. in response to heat stress. This contrasting expression of some Ca^{2+} homeostasis proteins in this study, compared to some cnidarian stress experiments that lead to lower calcification rates and survival, suggests that Calmodulin and acute calcium homeostasis disruption are involved in the rapid wound regeneration we observed.

6D. Antioxidant defenses

To preserve cellular function and survive stressful conditions, an organism must generate energy via oxidative phosphorylation, which leads to ROS accumulation. These ROS must be met with antioxidant molecules to avoid further damage of cellular DNA, proteins, and lipids (Scandalios, 2002). Oxidative stress has been shown to disrupt ionic balances within a cell and this is corroborated in this study by upregulation of a variety of ion transporters (Copper, Magnesium, zinc, Sodium/potassium-transporting ATPases) in response to both fragmentation and outplanting (Supplemental Table 1). Similar to results of other cnidarian stress experiments, this study found several antioxidant molecules (heat-shock proteins, thioredoxins, ferritin) (Supplemental Figure 4) as well as GO categories associated with cell-redox homeostasis (Pattern 1 of Figure 7) were upregulated in response to both fragmentation and outplanting. The thioredoxin redox system is a ubiquitous cellular repair mechanism that mediates the reduction of damaged protein disulfide bonds and are a major regulatory mechanism in cell redox signal transduction (Arnér & Holmgren, 2000). Ferritin controls the available ferrous iron (Fe^{2+}) inside the cell, which is associated with the generation of free radicals, and is upregulated in response to heat shock in corals (Desalvo et al., 2008; Császár et al., 2009; Bellantuono et al., 2012), as well as fragmentation in this present study. Ferritin levels in invertebrates are thought to be mainly

controlled by transcriptional regulation making it a potentially useful biomarker for stress because mRNA levels are likely representative of protein concentration (Torti & Torti, 2002; Császár et al., 2009) which is potentially not the case for other antioxidant molecules. The upregulation of genes that participate in the thioredoxin oxidoreductase system (thioredoxin, peroxiredoxin-1, Peptide-methionine (S)-S-oxide reductase (EC 1.8.4.11), and glutathione transferase), ferritin, and ion transporters in response to both fragmentation and outplanting further suggest significant increase in antioxidant and protein repair mechanisms to combat oxidative damage from increased energy production necessary for wound regeneration and survival.

Antioxidant molecules that were once thought of as unique biomarkers for heat stress, such as heat-shock proteins (HSPs), are now understood to be upregulated in response to a variety of stressors, including physical injury in this study. Several studies have suggested that the absence of a HSP response is linked with the initiation of apoptosis pathways (Feder & Hofmann, 1999; Gorman et al., 1999; Samali et al., 1999). Thus, the presence of upregulated HSPs indicate a push for survival. In response to physical injury in this study, *Porites lobata* colonies demonstrated a diverse upregulation of mitochondrial, cytosol, and ER resident HSPs (HSP70, HSP90, 95kDA HSP, 10kDA HSP, DnaJ-like HSP40s). Arguably the most studied and ubiquitous HSPs, HSP70 (Feder & Hofmann, 1999), was the strongest upregulated oxidative stress associated gene in response to fragmentation (\log_2FC 2.95; FDR $1.2e^{-9}$). Interestingly, Zhang & Horvath (2005) implicated HSP70, specifically, in cell proliferation and apoptosis-resistance in cancerous cells. HSP 10kDA and certain DnaJ-like proteins (HSP40) assist in protein folding activities within the mitochondria (Feder & Hofmann, 1999), and may help stabilize mitochondrial proteins during the increased energy production observed in response to

fragmentation. The upregulation of 97 kDA HSP in response to fragmentation and subsequent downregulation after two weeks of growth may suggest that oxidative damage to proteins begins to subside within 2wk after physical injury. Additionally, no antioxidant enzymes were found upregulated after two weeks or two months of growth, suggesting that the increased ROS, and therefore antioxidant demands, diminished within a few weeks of physical injury. Although the thioredoxin system and HSPs remain the most studied and indicative biomarkers for cellular oxidative stress, further study is required to understand their specific roles in protein folding, assembly, regulation, and degradation in cnidarians (Feder & Hofmann, 1999; Maor-Landaw & Levy, 2016).

6E. Protein turnover

The ER plays crucial roles in controlling protein quality, facilitating the degradation of misfolded proteins, and sensing homeostasis changes such as the release of Ca^{2+} into the cytosol. When significant protein damage occurs and calcium homeostasis disruption occurs, ER-stress pathways are stimulated leading to the increased protein stabilization, degradation, and synthesis required to preserve cellular function (Bahar et al., 2016). GO terms associated with amino acid catabolism (Pattern 2 of Figure 7) were down regulated in response to both stress events, which might suggest that amino acids are preserved during protein catabolism to provide the necessary building blocks for increased protein anabolism as corals undergo stress events (Klasing, 2009). The upregulation of GO terms associated with protein turnover (protein catabolism, anabolism, folding) (Pattern 1 of Figure 7), as well as specific protein stabilization and refolding chaperones (HSPs, thioredoxin, calreticulin and calumenin) and ubiquitin-associated degradation enzymes during both fragmentation and outplanting suggest significant ER stress (Supplemental Table 4). Interestingly, we did not find upregulation of specific ER-stress signal transducers known in

other organisms (inositol-requiring protein-1 (IRE1), activating transcription factor-6 (ATF6) or protein kinase RNA (PKR)-like ER kinase (PERK)) (Ron & Walter, 2007). However, Aguilar et al. 2019 found evidence of upregulation of PERK and ATF6 signal transduction systems after 24hr of hyposaline stress in *Acropora millepora*. Similar and related to calcium homeostasis disruption, the duration of ER-stress often determines if pro-survival or pro-apoptotic signaling will persist (Szegezdi et al., 2006; Bahar et al., 2016). The fact that ER-stress signal transducers are not upregulated 1 day after outplanting suggests that the fragments are already recovering from initial stress. Decrease rates of translation initiation is one of the earliest stages of ER stress, and yet we find significant upregulation of translation initiation factors (17/17) 1 day after fragmentation (Supplemental Table 4), which might suggest that the corals were already recovering from initial ER stress 1 day after fragmentation, and upregulating antioxidant defenses, protein stabilizing molecules, and, ultimately, rapid wound regeneration in a push for survival.

6F. Impacts of physical injury on the host-symbiont relationship

Decreased photosystem performance and the breakdown of coral-zooxanthellae symbiosis are known responses to various environmental stressors including heat shock (DeSalvo et al., 2010), ocean acidification (Anthony et al., 2008), darkness (DeSalvo et al., 2012), hypo-salinity (Downs et al., 2009; Ellison et al., 2017), and UV exposure (Tarrant et al., 2014), but remains uncharacterized in scleractinian corals response to physical disturbance. However, photosynthetic yield and zooxanthellae densities have been shown to be unaffected by fragmentation in soft coral (Rocha et al., 2013). The very small differences in relative gene expression (<10 genes) between timepoints within the symbiont (Table 1) and the absence of differentially expressed symbiont antioxidant genes suggests that the ROS are exclusively

produced within the host or are quickly transferred from the symbiont to the host. Additionally, we found no evidence of Nitric Oxide (NO) homeostasis breakdown within the host's response to physical fragmentation, which has been previously correlated with the breakdown of symbiosis in response to bleaching (Perez & Weis, 2006; DeSalvo et al., 2010; Maor-Landaw & Levy, 2016). Together these results suggest that the coral-zooxanthellae symbiosis is far less affected by fragmentation than it is by other environmental stressors. This may help maintain and increase symbiotic energy production necessary for cellular protein maintenance, antioxidant defense, and rapid wound regeneration. Assays of NO concentration within host cells undergoing physical injury would further determine if the host-symbiont relationship is maintained under this type of stress. Further study is required to understand the host-symbiont relationship under physical stress.

7. Conclusions

In this study on *Porites lobata* response to physical injury and outplanting stress, we observed many metabolic similarities to other cnidarian stress events, with some important differences. Environmental stress events in corals lead to decreased energy production (Maor-Landaw & Levy, 2016), lower calcification rates (Anthony et al., 2008; Crook et al., 2013; D'Olivo & McCulloch, 2017), and mortality (Peter W. Glynn, 1990). Our study found acute responses to physical injury that involved significantly increased energy production, phosphoinositide-mediated calcium homeostasis disruption, and ER stress leading to increased antioxidant expression and rates of protein turnover. We hypothesized that phosphoinositide-mediated acute calcium homeostasis disruption stimulates wound recovery processes and the rapid growth over cut margins observed in this study. The duration of ER stress and calcium homeostasis disruption often determines a cell's fate in response to environmental changes

(Orrenius et al., 2003; Bahar et al., 2016). The concurrent upregulation of calcium disruption and sequestering signals, translation initiation factors and ER stress-associated molecules (protein chaperones and ubiquitin-degradation enzymes), as well as heat shock proteins, in response to physical injury support our hypothesis that fragments are beginning to recover and pushing for survival. Half as many genes were present in response to outplanting as compared to fragmentation. Low gene expression differences between 2 wk and 2 mo of growth and partial bleaching of new tissue after outplanting suggest that growing corals past when their cut margins are sealed may not be beneficial. Although these are energetically costly processes, *Porites lobata* fragments were capable of rapid wound regeneration following physical disturbance and high survival under controlled conditions. This study provides insight into the physiological mechanisms that allow for rapid wound recovery and stabilization in response to physical injury in corals, which informs restoration efforts.

8. References:

- Aguilar, C., Raina, J. B., Fôret, S., Hayward, D. C., Lapeyre, B., Bourne, D. G., & Miller, D. J. (2019). Transcriptomic analysis reveals protein homeostasis breakdown in the coral *Acropora millepora* during hypo-saline stress. *BMC Genomics*, *20*(1), 1–13. <https://doi.org/10.1186/s12864-019-5527-2>
- Anderson, D. A., Walz, M. E., Weil, E., Tonellato, P., & Smith, M. C. (2016). RNA-Seq of the Caribbean reef-building coral *Orbicella faveolata* (Scleractinia-Merulinidae) under bleaching and disease stress expands models of coral innate immunity. *PeerJ*, *4*, e1616.

<https://doi.org/10.7717/peerj.1616>

- Anthony, K. R. N., Connolly, S. R., & Hoegh-Guldberg, O. (2007). Bleaching, energetics, and coral mortality risk: Effects of temperature, light, and sediment regime. *Limnology and Oceanography*, 52(2), 716–726. <https://doi.org/10.4319/lo.2007.52.2.0716>
- Anthony, K. R. N., Kline, D. I., Diaz-Pulido, G., Dove, S., & Hoegh-Guldberg, O. (2008). Ocean acidification causes bleaching and productivity loss in coral reef builders. *Proceedings of the National Academy of Sciences of the United States of America*, 105(45), 17442–17446. <https://doi.org/10.1073/pnas.0804478105>
- Arner, E. S. J., & Holmgren, A. (2000). Physiological functions of thioredoxin and thioredoxin reductase. *European Journal of Biochemistry*, 267(20), 6102–6109. <https://doi.org/10.1046/j.1432-1327.2000.01701.x>
- Ashburner, M., Ball, C., Blake, J., Botstein, D., Butler, H., Cherry, M., ... Sherlock, G. (2004). Gene Ontology: tool for the unification of biology David. *Hydrologie Und Wasserbewirtschaftung*, 48(1), 2–11. <https://doi.org/10.1038/75556.Gene>
- Bagur, R., & Hajnóczky, G. (2017). Intracellular Ca²⁺ Sensing: Its Role in Calcium Homeostasis and Signaling. *Molecular Cell*, 66(6), 780–788. <https://doi.org/10.1016/j.molcel.2017.05.028>
- Bahar, E., Kim, H., & Yoon, H. (2016). ER stress-mediated signaling: Action potential and Ca²⁺ as key players. *International Journal of Molecular Sciences*, 17(9), 1–22. <https://doi.org/10.3390/ijms17091558>
- Bak, R. P. M. (1983). Neoplasia, regeneration and growth in the reef-building coral *Acropora palmata*. *Marine Biology*, 77(3), 221–227. <https://doi.org/10.1007/BF00395810>
- Bak, R. P. M., & Meesters, E. H. (2002). Acclimatization/adaptation of coral reefs in a marginal environment, 1(October).
- Bak, R. P. M., & Yvonne, S.-V. E. (1980). Regeneration of Superficial Damage in the Scleractinian Corals *Agaricia Agaricites F. Purpurea* and *Porites Astreoides*. *Bulletin of Marine Science*, 30(4), 883–887. Retrieved from <http://www.ingentaconnect.com/content/umrsmas/bullmar/1980/00000030/00000004/art00010>
- Barshis, D. J., Ladner, J. T., Oliver, T. A., Seneca, F. O., Traylor-Knowles, N., & Palumbi, S. R. (2013). Genomic basis for coral resilience to climate change. *Proceedings of the National Academy of Sciences*, 110(4), 1387–1392. <https://doi.org/10.1073/pnas.1210224110>
- Barshis, D. J., Stillman, J. H., Gates, R. D., Toonen, R. J., Smith, L. W., & Birkeland, C. (2010). Protein expression and genetic structure of the coral *Porites lobata* in an environmentally extreme Samoan back reef: Does host genotype limit phenotypic plasticity? *Molecular Ecology*, 19(8), 1705–1720. <https://doi.org/10.1111/j.1365-294X.2010.04574.x>
- Barton, J. A., Willis, B. L., & Hutson, K. S. (2017). Coral propagation: a review of techniques for ornamental trade and reef restoration. *Reviews in Aquaculture*, 9(3), 238–256. <https://doi.org/10.1111/raq.12135>
- Baums, I. B. (2008). A restoration genetics guide for coral reef conservation. *Molecular Ecology*, 17(12), 2796–2811. <https://doi.org/10.1111/j.1365-294X.2008.03787.x>

- Bay, L. K., Guérécheau, A., Andreakis, N., Ulstrup, K. E., & Matz, M. V. (2013). Gene Expression Signatures of Energetic Acclimatisation in the Reef Building Coral *Acropora millepora*. *PLoS ONE*, 8(5), e61736. <https://doi.org/10.1371/journal.pone.0061736>
- Bay, R. A., & Palumbi, S. R. (2015). Rapid Acclimation Ability Mediated by Transcriptome Changes in Reef-Building Corals. *Genome Biology and Evolution*, 7(6), 1602–1612. <https://doi.org/10.1093/gbe/evv085>
- Bellantuono, A. J., Granados-Cifuentes, C., Miller, D. J., Hoegh-Guldberg, O., & Rodriguez-Lanetty, M. (2012). Coral Thermal Tolerance: Tuning Gene Expression to Resist Thermal Stress. *PLoS ONE*, 7(11), e50685. <https://doi.org/10.1371/journal.pone.0050685>
- Berridge, M. J., & Irvine, R. F. (1989). Inositol phosphates and cell signalling. *Nature*, 341(6239), 197–205. <https://doi.org/10.1038/341197a0>
- Bertucci, A., Tambutté, S., Supuran, C. T., Allemand, D., & Zoccola, D. (2011). A New Coral Carbonic Anhydrase in *Stylophora pistillata*. *Marine Biotechnology*, 13(5), 992–1002. <https://doi.org/10.1007/s10126-011-9363-x>
- Burdick, D., Brown, V., Asher, J., Gawel, M., Goldman, L., Hall, A., ... Zglickzynski, B. (2008). The State of Coral Reef Ecosystems of Guam. *The State of Coral Reef Ecosystems of the United States and Pacific Freely Associated States: 2008, Technical*, 465–510.
- Burns, N. M. (2018). USING SURVIVOR POPULATIONS TO MITIGATE BLEACHING MORTALITY OF STAGHORN ACROPORA CORALS.
- Carilli, J. E., Norris, R. D., Black, B. A., Walsh, S. M., & McField, M. (2009). Local stressors reduce coral resilience to bleaching. *PLoS ONE*, 4(7), 1–5. <https://doi.org/10.1371/journal.pone.0006324>
- Carpenter, K. E., Abrar, M., Aeby, G., Aronson, R. B., Banks, S., Bruckner, A., ... Wood, E. (2008). One-third of reef-building corals face elevated extinction risk from climate change and local impacts. *Science (New York, N.Y.)*, 321(5888), 560–563. <https://doi.org/10.1126/science.1159196>
- Chadwick-Furman, N. E., Goffredo, S., & Loya, Y. (2000). Growth and population dynamic model of the reef coral *Fungia granulosa* Klunzinger, 1879 at Eilat, northern Red Sea. *Journal of Experimental Marine Biology and Ecology*, 249(2), 199–218. [https://doi.org/10.1016/S0022-0981\(00\)00204-5](https://doi.org/10.1016/S0022-0981(00)00204-5)
- Crabbe, M. J. C., & Smith, D. J. (2005). Sediment impacts on growth rates of *Acropora* and *Porites* corals from fringing reefs of Sulawesi, Indonesia. *Coral Reefs*, 24(3), 437–441. <https://doi.org/10.1007/s00338-005-0004-6>
- Crook, E. D., Cohen, A. L., Rebolledo-Vieyra, M., Hernandez, L., & Paytan, A. (2013). Reduced calcification and lack of acclimatization by coral colonies growing in areas of persistent natural acidification. *Proceedings of the National Academy of Sciences*, 110(27), 11044–11049. <https://doi.org/10.1073/pnas.1301589110>
- Császár, N. B. M., Seneca, F. O., & Van Oppen, M. J. H. (2009). Variation in antioxidant gene expression in the scleractinian coral *Acropora millepora* under laboratory thermal stress. *Marine Ecology Progress Series*, 392(May 2014), 93–102. <https://doi.org/10.3354/meps08194>
- D’Olivo, J. P., & McCulloch, M. T. (2017). Response of coral calcification and calcifying fluid composition to thermally induced bleaching stress. *Scientific Reports*, 7(1), 1–15. <https://doi.org/10.1038/s41598-017-02306-x>

- Darling, E. S., Alvarez-Filip, L., Oliver, T. A., Mcclanahan, T. R., & Côté, I. M. (2012). Evaluating life-history strategies of reef corals from species traits. *Ecology Letters*, *15*(12), 1378–1386. <https://doi.org/10.1111/j.1461-0248.2012.01861.x>
- DeSalvo, M. K., Estrada, A., Sunagawa, S., & Medina, M. (2012). Transcriptomic responses to darkness stress point to common coral bleaching mechanisms. *Coral Reefs*, *31*(1), 215–228. <https://doi.org/10.1007/s00338-011-0833-4>
- DeSalvo, M. K., Sunagawa, S., Voolstra, C., & Medina, M. (2010). Transcriptomic responses to heat stress and bleaching in the elkhorn coral *Acropora palmata*. *Marine Ecology Progress Series*, *402*, 97–113. <https://doi.org/10.3354/meps08372>
- Desalvo, M. K., Voolstra, C. R., Sunagawa, S., Schwarz, J. A., Stillman, J. H., Coffroth, M. A., ... Medina, M. (2008). Differential gene expression during thermal stress and bleaching in the Caribbean coral *Montastraea faveolata*. *Molecular Ecology*, *17*(17), 3952–3971. <https://doi.org/10.1111/j.1365-294X.2008.03879.x>
- Dodge, R. E., Aller, R. C., & Thompson, J. (1974). Coral Growth Related to Resuspension of Bottom Sediment. *Nature*.
- Done, T. J., & Potts, D. C. (1992). Influences of habitat and natural disturbances on contributions of massive *Porites* corals to reef communities. *Marine Biology*, *114*(3), 479–493. <https://doi.org/10.1007/BF00350040>
- Downs, C. A., Kramarsky-Winter, E., Woodley, C. M., Downs, A., Winters, G., Loya, Y., & Ostrander, G. K. (2009). Cellular pathology and histopathology of hypo-salinity exposure on the coral *Stylophora pistillata*. *Science of the Total Environment*, *407*(17), 4838–4851. <https://doi.org/10.1016/j.scitotenv.2009.05.015>
- Edmunds, P. J., & Gates, R. D. (1999). The Physiological Mechanisms of Acclimatization in Tropical Reef Corals. *American Zoologist*, *39*(1), 30–43. <https://doi.org/10.1093/icb/39.1.30>
- Edmunds, P. J., & Gates, R. D. (2008). Acclimatization in tropical reef corals. *Marine Ecology Progress Series*, *361*, 307–310. <https://doi.org/10.3354/meps07556>
- Edwards, A. J. (2008). *Reef Rehabilitation Manual. Coral Reef Targeted Research & Capacity Building for Management Program: St Lucia, Australia. Construction* (Vol. 501). The Coral Reef Targeted Research & Capacity Building for Management Program.
- Edwards, A. J., & Clark, S. (1999). Coral transplantation: a useful management tool or misguided meddling? *Marine Pollution Bulletin*, *37*(8–12), 474–487.
- Edwards, A. J., & Gomez, E. D. (2011). Reef Restoration Concepts and Guidelines: making sensible management choices in the face of uncertainty. *Encyclopedia of Earth Sciences Series, Part 2*, 889–896. https://doi.org/10.1007/978-90-481-2639-2_140
- Ellison, M. A., Ferrier, M. D., & Carney, S. L. (2017). Salinity stress results in differential Hsp70 expression in the *Exaiptasia pallida* and *Symbiodinium* symbiosis. *Marine Environmental Research*, *132*(October), 63–67. <https://doi.org/10.1016/j.marenvres.2017.10.006>
- Epstein, N., & Bak, R. P. M. (2016). Strategies for Gardening Denuded Coral Reef Areas : The Applicability of Using Different Types of Coral Material for Reef ... Strategies for Gardening Denuded Coral Reef Areas : The Applicability of Using Different Types of Coral Material for Reef Restora, *9*(November),

432–442. <https://doi.org/10.1046/j.1526-100X.2001.94012.x>

- Epstein, N., Bak, R. P. M., & Rinkevich, B. (2003). Applying forest restoration principles to coral reef rehabilitation. *Aquatic Conservation: Marine and Freshwater Ecosystems*, *13*(5), 387–395. <https://doi.org/10.1002/aqc.558>
- Feder, M. E., & Hofmann, G. E. (1999). Heat-shock proteins, molecular chaperones, and the stress response: Evolutionary and ecological physiology. *Annual Review of Physiology*, *61*, 243–282. <https://doi.org/10.1146/annurev.physiol.61.1.243>
- Fifer, J. (2018). DETERMINING THE EFFECT OF HYDRODYNAMICS ON REDUCING HEAT STRESS IN STAGHORN CORAL.
- Forsman, Z. H., Page, C. A., Toonen, R. J., & Vaughan, D. (2015). Growing coral larger and faster: micro-colony-fusion as a strategy for accelerating coral cover. *PeerJ*, *3*, e1313. <https://doi.org/10.7717/peerj.1313>
- Forsman, Z. H., Rinkevich, B., & Hunter, C. L. (2006). Investigating fragment size for culturing reef-building corals (*Porites lobata* and *P. compressa*) in ex situ nurseries. <https://doi.org/10.1016/j.aquaculture.2006.06.040>
- Franssen, S. U., Gu, J., Bergmann, N., Winters, G., Klostermeier, U. C., Rosenstiel, P., ... Reusch, T. B. H. (2011). Transcriptomic resilience to global warming in the seagrass *Zostera marina*, a marine foundation species. *Proceedings of the National Academy of Sciences*, *108*(48), 19276–19281. <https://doi.org/10.1073/pnas.1107680108>
- Ganot, P., Moya, A., Magnone, V., Allemand, D., Furla, P., & Sabourault, C. (2011). Adaptations to endosymbiosis in a Cnidarian-Dinoflagellate association: Differential gene expression and specific gene duplications. *PLoS Genetics*, *7*(7). <https://doi.org/10.1371/journal.pgen.1002187>
- Glynn, P. W. (1993). Coral reef bleaching: ecological perspectives. *Coral Reefs*, *12*(1), 1–17. <https://doi.org/10.1007/BF00303779>
- Glynn, Peter W. (1990). Coral Mortality and Disturbances to Coral Reefs in the Tropical Eastern Pacific. *Elsevier Oceanography Series*, *52*(C), 55–126. [https://doi.org/10.1016/S0422-9894\(08\)70033-3](https://doi.org/10.1016/S0422-9894(08)70033-3)
- Goreau, T. J., & Hilbertz, W. (2005). Marine Ecosystems Restoration: Costs And Benefits For Coral Reefs. *World Resource Review*, *17*(3), 375–409.
- Gorman, A. M., Heavey, B., Creagh, E., Cotter, T. G., & Samali, A. (1999). Antioxidant-mediated inhibition of the heat shock response leads to apoptosis. *FEBS Letters*, *445*(1), 98–102. [https://doi.org/10.1016/S0014-5793\(99\)00094-0](https://doi.org/10.1016/S0014-5793(99)00094-0)
- Grabherr, M. G., Haas, B. J., Yassour, M., Levin, J. Z., Thompson, D. A., Amit, I., ... Regev, A. (2013). Trinity: reconstructing a full-length transcriptome without a genome from RNA-Seq data. *Nature Biotechnology*, *29*(7), 644–652. <https://doi.org/10.1038/nbt.1883.Trinity>
- Haas, B. J., Papanicolaou, A., Yassour, M., Grabherr, M., Blood, P. D., Bowden, J., ... Regev, A. (2013). De novo transcript sequence reconstruction from RNA-seq using the Trinity platform for reference generation and analysis. *Nature Protocols*, *8*(8), 1494–1512. <https://doi.org/10.1038/nprot.2013.084>
- Harrison, P. L., & Wallace, C. C. (1990). A review of reproduction, larval dispersal and settlement of

- scleractinian corals. In *Chapter 7 in Ecosystems of the World 25 Coral Reefs* (ed. Z. Dubinsky). (pp. 133–196). Retrieved from https://www.researchgate.net/publication/304784746_Harrison_PL_and_Wallace_C_C_1990_A_review_of_reproduction_larval_dispersal_and_settlement_of_scleractinian_corals_Chapter_7_in_Ecosystems_of_the_World_25_Coral_Reefs_ed_Z_Dubinsky_Amsterdam_Elsevier_p
- Hawkins, J. P., & Roberts, C. M. (1993). Effects of Recreational Scuba Diving on Coral Reefs: Trampling on Reef-Flat Communities. *The Journal of Applied Ecology*, 30(1), 25. <https://doi.org/10.2307/2404267>
- Helen, T. Y. (2000). The case for restoration of tropical coastal ecosystems. *Ocean and Coastal Management*, 43(8–9), 841–851.
- Herlan, J., & Lirman, D. (2008). Development of a coral nursery program for the threatened coral *Acropora cervicornis* in Florida. *Proceedings of the 11th International Coral Reef Symposium*, 24(24), 1244–1247. Retrieved from <http://www.nova.edu/ncri/11icrs/proceedings/files/m24-11.pdf>
- Highsmith, R. (2007). Reproduction by Fragmentation in Corals. *Marine Ecology Progress Series*, 7, 207–226. <https://doi.org/10.3354/meps007207>
- Hodgson, G. (1990). Sediment and the settlement of larvae of the reef coral *Pocillopora damicornis*. *Coral Reefs*, 9(1), 41–43. <https://doi.org/10.1007/BF00686720>
- Hoegh-Guldberg, O., Mumby, P. J., Hooten, A. J., Steneck, R. S., Greenfield, P., Gomez, E., ... Hatzioiols, M. E. (2007). Coral reefs under rapid climate change and ocean acidification. *Science (New York, N.Y.)*, 318(5857), 1737–1742. <https://doi.org/10.1126/science.1152509>
- Hoot, W. C. (2019). Guam Coral Reef Resilience Strategy, (December).
- Huang, Y., Yuan, J., Zhang, Y., Peng, H., & Liu, L. (2018). Molecular cloning and characterization of calmodulin-like protein CaLP from the Scleractinian coral *Galaxea astreata*. *Cell Stress and Chaperones*, 23(6), 1329–1335. <https://doi.org/10.1007/s12192-018-0907-0>
- Hugees, T. P. (1985). Life Histories and Population Dynamics of Early Successional Corals. *Proceedings of the Fifth International Coral Reef Congress*, 4. Retrieved from https://researchonline.jcu.edu.au/25777/1/Hughes_1986.pdf
- Hughes, T. P. (1989). Community Structure and Diversity of Coral Reefs : The Role of History. *Ecology*, 70(1), 275–279.
- Hughes, T. P., & Connell, J. H. (1987). Population Dynamics Based on Size or Age ? A Reef-Coral Analysis, 129(6), 818–829.
- Hughes, T. P., & Jackson, J. B. C. (1980). Do corals lie about their age? Some demographic consequences of partial mortality, fission, and fusion. *Science*, 209(4457), 713–715. <https://doi.org/10.1126/science.209.4457.713>
- Johansen, S. D., Emblem, Å., Karlsen, B. O., Okkenhaug, S., Hansen, H., Moum, T., ... Seternes, O. M. (2010). Approaching marine bioprospecting in hexacorals by RNA deep sequencing. *New Biotechnology*, 27(3), 267–275. <https://doi.org/10.1016/j.nbt.2010.02.019>
- Jones, A. M., Berkelmans, R., Van Oppen, M. J. H., Mieog, J. C., & Sinclair, W. (2008). A community change in the algal endosymbionts of a scleractinian coral following a natural bleaching event: Field

- evidence of acclimatization. *Proceedings of the Royal Society B: Biological Sciences*, 275(1641), 1359–1365. <https://doi.org/10.1098/rspb.2008.0069>
- Kenkel, C. D., Goodbody-Gringley, G., Caillaud, D., Davies, S. W., Bartels, E., & Matz, M. V. (2013). Evidence for a host role in thermotolerance divergence between populations of the mustard hill coral (*Porites astreoides*) from different reef environments. *Molecular Ecology*, 22(16), 4335–4348. <https://doi.org/10.1111/mec.12391>
- Klasing, K. C. (2009). Minimizing amino acid catabolism decreases amino acid requirements. *Journal of Nutrition*, 139(1), 11–12. <https://doi.org/10.3945/jn.108.099341>
- Kojis, B. L., & Quinn, N. J. (1981). Reproductive strategies in four species of *Porites* (Scleractinia). *Fourth International Coral Reef Symposium, Manila*, (August), 145–151.
- Kojis, B. L., & Quinn, N. J. (2001). The importance of regional differences in hard coral recruitment rates for determining the need for coral restoration. *Bulletin of Marine Science*, 69(2), 967–974. <https://doi.org/10.1098/rsbl.2003.0087>
- Koop, K., Booth, D., Broadbent, A., Brodie, J., Bucher, D., Capone, D., ... Yellowlees, D. (2001). ENCORE: the effect of nutrient enrichment on coral reefs. Synthesis of results and conclusions. *Marine Pollution Bulletin*, 42(2), 91–120. Retrieved from <http://www.ncbi.nlm.nih.gov/pubmed/11381890>
- Kozłowski, J., & Wiegert, R. G. (1986). Optimal allocation of energy to growth and reproduction. *Theoretical Population Biology*, 29(1), 16–37. [https://doi.org/10.1016/0040-5809\(86\)90003-1](https://doi.org/10.1016/0040-5809(86)90003-1)
- Lajeunesse, T. C., Parkinson, J. E., Gabrielson, P. W., Jeong, H. J., Reimer, J. D., Voolstra, C. R., & Santos, S. R. (2018). Systematic Revision of Symbiodiniaceae Highlights the Antiquity and Diversity of Coral Endosymbionts. *Current Biology*, 28(16), 2570-2580.e6. <https://doi.org/10.1016/j.cub.2018.07.008>
- Lapacek, V. A. (2017). SEXUAL REPRODUCTIVE BIOLOGY OF GUAM'S STAGHORN ACROPORA.
- Lewis, R. (2016). Wetlands restoration / creation / enhancement terminology : Suggestions for standardization, (January 1990).
- Lirman, D. (2000). Fragmentation in the branching coral *Acropora palmata* (Lamarck): Growth, survivorship, and reproduction of colonies and fragments. *Journal of Experimental Marine Biology and Ecology*, 251(1), 41–57. [https://doi.org/10.1016/S0022-0981\(00\)00205-7](https://doi.org/10.1016/S0022-0981(00)00205-7)
- Lirman, D. (2012). a Review of Reef Restoration and Coral Propagation Using the Threatened Genus *Acropora* in the Caribbean and Western Atlantic, 88(4), 1075–1098. Retrieved from <https://www.ingentaconnect.com/content/umrsmas/bullmar/2012/00000088/00000004/art00016?crawler=true&mimetype=application/pdf>
- Lirman, D., Thyberg, T., Herlan, J., Hill, C., Young-Lahiff, C., Schopmeyer, S., ... Drury, C. (2010). Propagation of the threatened staghorn coral *Acropora cervicornis*: Methods to minimize the impacts of fragment collection and maximize production. *Coral Reefs*, 29(3), 729–735. <https://doi.org/10.1007/s00338-010-0621-6>
- Lough, J. M., & Barnes, D. J. (2000). Environmental controls on growth of the massive coral *Porites*. *Journal of Experimental Marine Biology and Ecology*, 245(2), 225–243. [https://doi.org/10.1016/S0022-0981\(99\)00168-9](https://doi.org/10.1016/S0022-0981(99)00168-9)
- Loya, Y., Sakai, K., Yamazato, K., Nakano, Y., Sambali, H., & van Woesik, R. (2001). Coral bleaching: the

- winners and the losers. *Ecology Letters*, 4(2), 122–131. <https://doi.org/10.1046/j.1461-0248.2001.00203.x>
- Lozada-Misa, P., Kerr, A., & Raymundo, L. (2015). Contrasting lesion dynamics of white syndrome among the scleractinian corals *Porites* spp. *PLoS ONE*, 10(6), 1–14. <https://doi.org/10.1371/journal.pone.0129841>
- Manzello, D. P., Matz, M. V., Enochs, I. C., Valentino, L., Carlton, R. D., Kolodziej, G., ... Jankulak, M. (2019). Role of host genetics and heat-tolerant algal symbionts in sustaining populations of the endangered coral *Orbicella faveolata* in the Florida Keys with ocean warming. *Global Change Biology*, 25(3), 1016–1031. <https://doi.org/10.1111/gcb.14545>
- Maor-Landaw, K., & Levy, O. (2016). Survey of Cnidarian Gene Expression Profiles in Response to Environmental Stressors: Summarizing 20 Years of Research, What Are We Heading for? In *The Cnidaria, Past, Present and Future* (pp. 523–543). <https://doi.org/10.1007/978-3-319-31305-4>
- Martin, M. (2011). Cutadapt removes adapter sequences from high-throughput sequencing reads. *EMBnet J Technical Notes*, 17(10), 2803–2809. <https://doi.org/doi:https://doi.org/10.14806/ej.17.1.200>
- McClanahan, T. R., Maina, J., Moothien-Pillay, R., & Baker, A. C. (2005). Effects of geography, taxa, water flow, and temperature variation on coral bleaching intensity in Mauritius. *Marine Ecology Progress Series*, 298, 131–142. <https://doi.org/10.3354/meps298131>
- Meesters, E. H., Noordeloos, M., & Bak, R. P. M. (1994). Damage and regeneration: Links to growth in the reef-building coral *Montastrea annularis*. *Marine Ecology Progress Series*, 112(1–2), 119–128. <https://doi.org/10.3354/meps112119>
- Moberg, F., & Folke, C. (1999). Ecological goods and services of coral reef ecosystems. *Ecological Economics*, 29(2), 215–233. [https://doi.org/10.1016/S0921-8009\(99\)00009-9](https://doi.org/10.1016/S0921-8009(99)00009-9)
- Nugues, M. M., & Roberts, C. M. (2003). Coral mortality and interaction with algae in relation to sedimentation. *Coral Reefs*, 22(4), 507–516. <https://doi.org/10.1007/s00338-003-0338-x>
- Oakley, C. A., & Davy, S. K. (2018). Cell Biology of Coral Bleaching, 189–211. https://doi.org/10.1007/978-3-319-75393-5_8
- Oakley, C. A., Durand, E., Wilkinson, S. P., Peng, L., Weis, V. M., Grossman, A. R., & Davy, S. K. (2017). Thermal Shock Induces Host Proteostasis Disruption and Endoplasmic Reticulum Stress in the Model Symbiotic Cnidarian *Aiptasia*. *Journal of Proteome Research*, 16(6), 2121–2134. <https://doi.org/10.1021/acs.jproteome.6b00797>
- Okubo, N., Motokawa, T., & Omori, M. (2007). When fragmented coral spawn? Effect of size and timing on survivorship and fecundity of fragmentation in *Acropora formosa*. *Marine Biology*, 151(1), 353–363. <https://doi.org/10.1007/s00227-006-0490-2>
- Okubo, N., Taniguchi, H., & Motokawa, T. (2005). Successful methods for transplanting fragments of *Acropora formosa* and *Acropora hyacinthus*. *Coral Reefs*, 24(2), 333–342. <https://doi.org/10.1007/s00338-005-0496-0>
- Oren, U., Benayahu, Y., Lubinevsky, H., & Loya, Y. (2012). Colony Integration during Regeneration in the Stony Coral *Favia fava*, 82(3), 802–813.

- Oren, U., Rinkevich, B., & Loya, Y. (1997). Oriented intra-colonial transport of ¹⁴C labeled materials during coral regeneration. *Marine Ecology Progress Series*, *161*(1989), 117–122. <https://doi.org/10.3354/meps161117>
- Orrenius, S., Zhivotovsky, B., & Nicotera, P. (2003). Regulation of cell death: The calcium-apoptosis link. *Nature Reviews Molecular Cell Biology*, *4*(7), 552–565. <https://doi.org/10.1038/nrm1150>
- Page, C. A., Muller, E. M., & Vaughan, D. E. (2018). Microfragmenting for the successful restoration of slow growing massive corals. *Ecological Engineering*, *123*, 86–94. <https://doi.org/10.1016/j.ecoleng.2018.08.017>
- Palmer, C. V., McGinty, E. S., Cummings, D. J., Smith, S. M., Bartels, E., & Mydlarz, L. D. (2011). Patterns of coral ecological immunology: variation in the responses of Caribbean corals to elevated temperature and a pathogen elicitor. *Journal of Experimental Biology*, *214*(24), 4240–4249. <https://doi.org/10.1242/jeb.061267>
- Palmer, C. V., Mydlarz, L. D., & Willis, B. L. (2008). Evidence of an inflammatory-like response in non-normally pigmented tissues of two scleractinian corals. *Proceedings of the Royal Society B: Biological Sciences*, *275*(1652), 2687–2693. <https://doi.org/10.1098/rspb.2008.0335>
- Palumbi, S. R., Barshis, D. J., & Bay, R. A. (2014). Mechanisms of reef coral resistance to future climate change. *344*(6186), 895–898.
- Palumbi, S. R., & Jackson, J. B. C. (1982). Ecology of cryptic coral reef communities. II. Recovery from small disturbance events by encrusting bryozoa: The influence of “host” species and lesion size. *Journal of Experimental Marine Biology and Ecology*, *64*(2), 103–115. [https://doi.org/10.1016/0022-0981\(82\)90147-2](https://doi.org/10.1016/0022-0981(82)90147-2)
- Pavey, S. A., Bernatchez, L., Aubin-Horth, N., & Landry, C. R. (2012). What is needed for next-generation ecological and evolutionary genomics? *Trends in Ecology & Evolution*, *27*(12), 673–678. <https://doi.org/10.1016/J.TREE.2012.07.014>
- Perez, S., & Weis, V. (2006). Nitric oxide and cnidarian bleaching: An eviction notice mediates breakdown of a symbiosis. *Journal of Experimental Biology*, *209*(14), 2804–2810. <https://doi.org/10.1242/jeb.02309>
- Pimentel, H., Bray, N. L., Puente, S., Melsted, P., & Pachter, L. (2017). Differential analysis of RNA-seq incorporating quantification uncertainty. *Nature Methods*, *14*(7), 687–690. <https://doi.org/10.1038/nmeth.4324>
- Pinzon, J. H., Kamel, B., Burge, C. A., Harvell, C. D., Medina, M., Weil, E., & Mydlarz, L. D. (2015). Whole transcriptome analysis reveals changes in expression of immune-related genes during and after bleaching in a reef-building coral. *Royal Society Open Science*, *2*(4), 140214–140214. <https://doi.org/10.1098/rsos.140214>
- Pinzón, J. H., Kamel, B., Burge, C. A., Harvell, C. D., Medina, M., Weil, E., & Mydlarz, L. D. (2015). Whole transcriptome analysis reveals changes in expression of immune-related genes during and after bleaching in a reef-building coral. *Royal Society Open Science*, *2*(4). <https://doi.org/10.1098/rsos.140214>
- Potts, D., Done, T., Isdale, P., & Fisk, D. (2007). Dominance of a coral community by the genus *Porites* (Scleractinia). *Marine Ecology Progress Series*, *23*, 79–84. <https://doi.org/10.3354/meps023079>

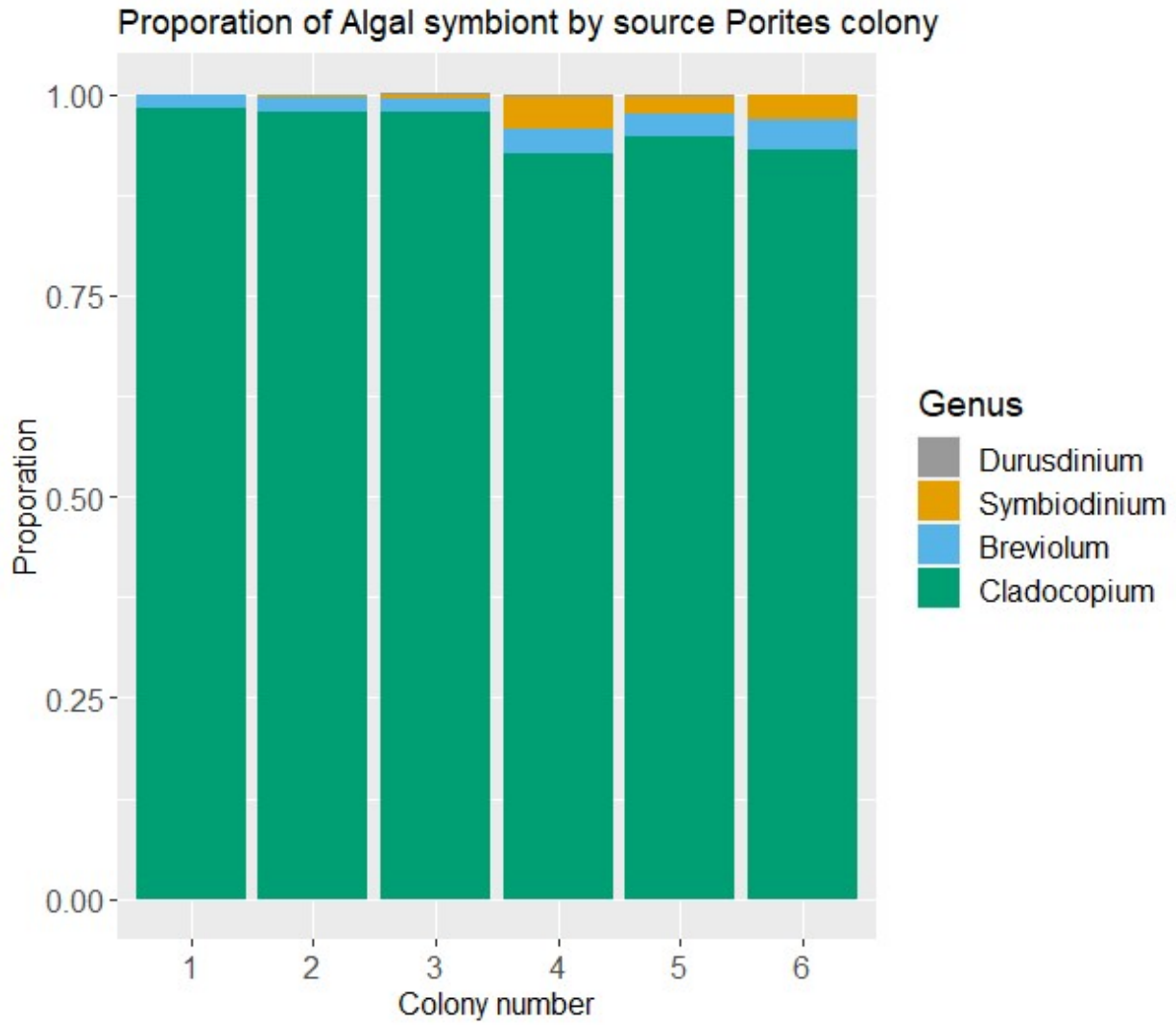
- Pratchett, M. S., Caballes, C. F., Wilmes, J. C., Matthews, S., Mellin, C., Sweatman, H. P. A., ... Uthicke, S. (2017). Thirty years of research on crown-of-thorns starfish (1986-2016): Scientific advances and emerging opportunities. *Diversity*, *9*(4). <https://doi.org/10.3390/d9040041>
- Raymundo, L. J., Burdick, D., Hoot, W. C., Miller, R. M., Brown, V., Reynolds, T., ... Williams, A. (2019). Successive bleaching events cause mass coral mortality in Guam, Micronesia. *Coral Reefs*. <https://doi.org/10.1007/s00338-019-01836-2>
- Raymundo, L. J., Burdick, D., Lapacek, V., Miller, R., & Brown, V. (2017). Anomalous temperatures and extreme tides: Guam staghorn *Acropora* succumb to a double threat. *Marine Ecology Progress Series*, *564*, 47–55. <https://doi.org/10.3354/meps12005>
- Raymundo, L. J., & Maypa, A. p. (2004). Getting Bigger Faster : Mediation of Size-Specific Mortality via Fusion in Juvenile Coral Transplants. *Ecological Society of America*, *14*(1), 281–295.
- Redding, J. E., Myers-Miller, R. L., Baker, D. M., Fogel, M., Raymundo, L. J., & Kim, K. (2013). Link between sewage-derived nitrogen pollution and coral disease severity in Guam. *Marine Pollution Bulletin*, *73*(1), 57–63. <https://doi.org/10.1016/j.marpolbul.2013.06.002>
- Reyes-Bermudez, A., Miller, D. J., & Sprungala, S. (2012). The Neuronal Calcium Sensor Protein Acrocalcin: A Potential Target of Calmodulin Regulation during Development in the Coral *Acropora millepora*. *PLoS ONE*, *7*(12). <https://doi.org/10.1371/journal.pone.0051689>
- Reyes-Bermudez, A., Villar-Briones, A., Ramirez-Portilla, C., Hidaka, M., & Mikheyev, A. S. (2016). Developmental progression in the coral *Acropora digitifera* is controlled by differential expression of distinct regulatory gene networks. *Genome Biology and Evolution*, *8*(3), 851–870. <https://doi.org/10.1093/gbe/evw042>
- Reynolds, T., Burdick, D., Houk, P., Raymundo, L. J., & Johnson, S. (2014). Unprecedented coral bleaching across the Marianas Archipelago. *Coral Reefs*, *33*(2), 499–499. <https://doi.org/10.1007/s00338-014-1139-0>
- Rinkevich, B. (1995). Restoration strategies for coral reefs damaged by recreational activities: the use of sexual and asexual recruits. *Restoration Ecology*.
- Rinkevich, B. (2005). Conservation of Coral Reefs through Active Restoration Measures: Recent Approaches and Last Decade Progress. <https://doi.org/10.1021/ES0482583>
- Rocha, R. J. M., Serôdio, J., Leal, M. C., Cartaxana, P., & Calado, R. (2013). Effect of light intensity on post-fragmentation photobiological performance of the soft coral *Sinularia flexibilis*. *Aquaculture*, *388–391*(1), 24–29. <https://doi.org/10.1016/j.aquaculture.2013.01.013>
- Ron, D., & Walter, P. (2007). Signal integration in the endoplasmic reticulum unfolded protein response. *Nature Reviews Molecular Cell Biology*, *8*(7), 519–529. <https://doi.org/10.1038/nrm2199>
- Ruesink, J. L. (1997). Coral injury and recovery: Matrix models link process to pattern. *Journal of Experimental Marine Biology and Ecology*, *210*(2), 187–208. [https://doi.org/10.1016/S0022-0981\(96\)02655-X](https://doi.org/10.1016/S0022-0981(96)02655-X)
- Ryan, J. (2014). Alien Index: identify potential non-animal transcripts or horizontally transferred genes in animal transcriptomes. <https://doi.org/http://dx.doi.org/10.5281/zenodo.21029>
- Samali, A., Holmberg, C. I., Sistonen, L., & Orrenius, S. (1999). Thermotolerance and cell death are

- distinct cellular responses to stress: Dependence on heat shock proteins. *FEBS Letters*, 461(3), 306–310. [https://doi.org/10.1016/S0014-5793\(99\)01486-6](https://doi.org/10.1016/S0014-5793(99)01486-6)
- Scandalios, J. G. (2002). Oxidative stress responses - What have genome-scale studies taught us? *Genome Biology*, 3(7), 1–6. <https://doi.org/10.1186/gb-2002-3-7-reviews1019>
- Schulz, F., Eloë-Fadrosch, E. A., Bowers, R. M., Jarett, J., Nielsen, T., Ivanova, N. N., ... Woyke, T. (2017). Towards a balanced view of the bacterial tree of life. *Microbiome*, 5(1), 140. <https://doi.org/10.1186/s40168-017-0360-9>
- Sealfon, S. C., & Chu, T. T. (2011). *Biological Microarrays* (Vol. 671). <https://doi.org/10.1007/978-1-59745-551-0>
- Seneca, F. O., & Palumbi, S. R. (2015). The role of transcriptome resilience in resistance of corals to bleaching. *Molecular Ecology*, 24(7), 1467–1484. <https://doi.org/10.1111/mec.13125>
- Simão, F. A., Waterhouse, R. M., Ioannidis, P., Kriventseva, E. V., & Zdobnov, E. M. (2015). BUSCO: Assessing genome assembly and annotation completeness with single-copy orthologs. *Bioinformatics*, 31(19), 3210–3212. <https://doi.org/10.1093/bioinformatics/btv351>
- Smith, & Hughes, T. P. (1999). Experimental assessment of coral fragments, 235, 147–164.
- Smith, L. W., Barshis, D. J., & Birkeland, C. (2007). Phenotypic plasticity for skeletal growth, density and calcification of *Porites lobata* in response to habitat type. *Coral Reefs*, 26(3), 559–567. <https://doi.org/10.1007/s00338-007-0216-z>
- Smith, Taylor, M., Nemeth, R. S., Brandt, M. E., Rothenberger, P., Kadison, E., ... Blondeau, J. (2013). Convergent mortality responses of Caribbean coral species to seawater warming. *Ecosphere*, 4(7), art87. <https://doi.org/10.1890/es13-00107.1>
- Soong, K. (1993). Colony size as a species character in massive reef corals. *Coral Reefs*, 12(2), 77–83. <https://doi.org/10.1007/BF00302106>
- Spalding, M., Burke, L., Wood, S. A., Ashpole, J., Hutchison, J., & zu Ermgassen, P. (2017). Mapping the global value and distribution of coral reef tourism. *Marine Policy*, 82(May), 104–113. <https://doi.org/10.1016/j.marpol.2017.05.014>
- Spurgeon, G. (2001). Improving the economic effectiveness of coral reef restoration. *Bulletin of Marine Science*, 69(2), 1031–1045.
- Stefan, C. J. (2020). Endoplasmic reticulum–plasma membrane contacts: Principals of phosphoinositide and calcium signaling. *Current Opinion in Cell Biology*, 63, 125–134. <https://doi.org/10.1016/j.ceb.2020.01.010>
- Supek, F., Bošnjak, M., Škunca, N., & Šmuc, T. (2011). Revigo summarizes and visualizes long lists of gene ontology terms. *PLoS ONE*, 6(7). <https://doi.org/10.1371/journal.pone.0021800>
- Szegezdi, E., Logue, S. E., Gorman, A. M., & Samali, A. (2006). Mediators of endoplasmic reticulum stress-induced apoptosis. *EMBO Reports*, 7(9), 880–885. <https://doi.org/10.1038/sj.embor.7400779>
- Tarasov, A. I., Griffiths, E. J., & Rutter, G. A. (2012). Regulation of ATP production by mitochondrial Ca²⁺. *Cell Calcium*, 52(1), 28–35. <https://doi.org/10.1016/j.ceca.2012.03.003>
- Tarrant, A. M., Reitzel, A. M., Kwok, C. K., & Jenny, M. J. (2014). Activation of the cnidarian oxidative

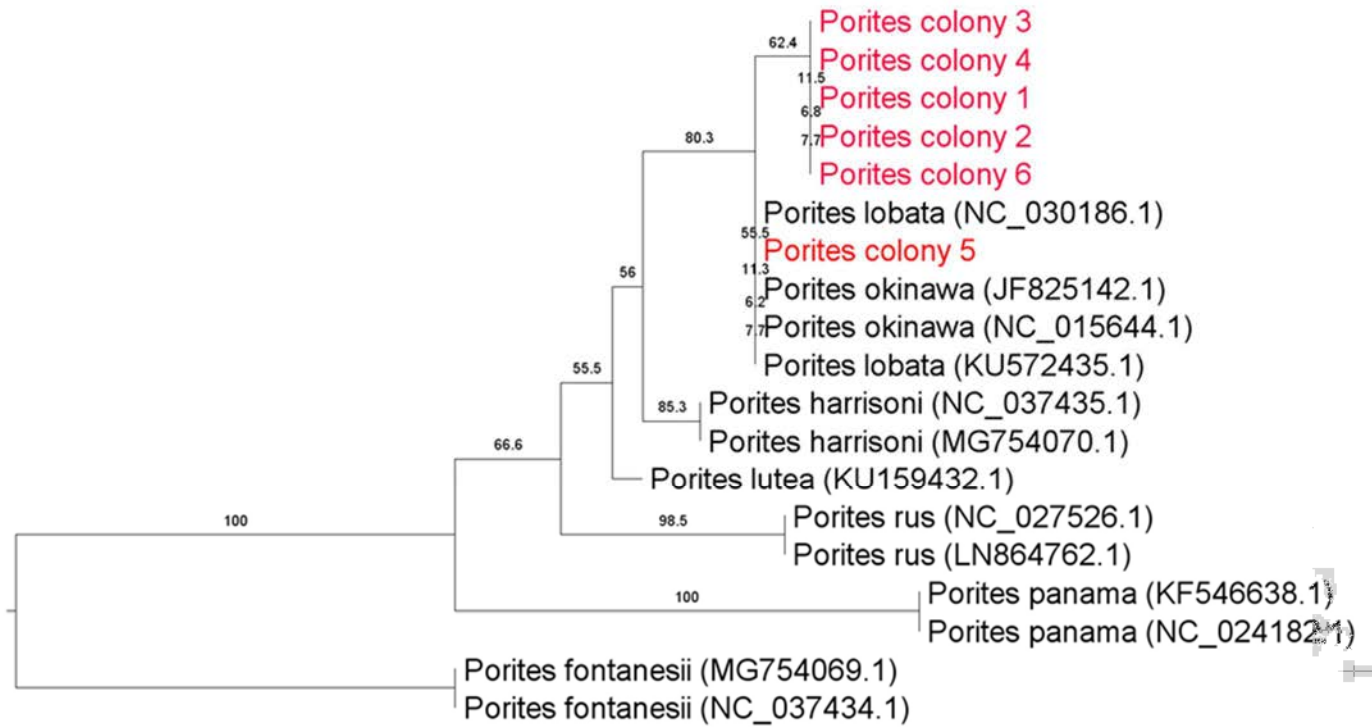
- stress response by ultraviolet radiation, polycyclic aromatic hydrocarbons and crude oil. *Journal of Experimental Biology*, 217(9), 1444–1453. <https://doi.org/10.1242/jeb.093690>
- Thomas, L., López, E. H., Morikawa, M. K., & Palumbi, S. R. (2019). *Transcriptomic resilience, symbiont shuffling, and vulnerability to recurrent bleaching in reef-building corals*. *Molecular Ecology*. <https://doi.org/10.1111/mec.15143>
- Thorhaug, A. (2011). Review of Seagrass Restoration efforts. *Ambio*, 15(2), 110–117.
- Torti, F. M., & Torti, S. V. (2002). Regulation of ferritin genes and protein. *Blood*, 99(10), 3505–3516. <https://doi.org/10.1182/blood.V99.10.3505>
- Van Woosik, R. (1998). Lesion healing on massive *Porites* spp. corals. *Marine Ecology Progress Series*, 164, 213–220. <https://doi.org/10.3354/meps164213>
- Veal, E. A., Mark Toone, W., Jones, N., & Morgan, B. A. (2002). Distinct roles for glutathione S-transferases in the oxidative stress response in *Schizosaccharomyces pombe*. *Journal of Biological Chemistry*, 277(38), 35523–35531. <https://doi.org/10.1074/jbc.M111548200>
- Vega Thurber, R. L., Burkepile, D. E., Fuchs, C., Shantz, A. A., Mcminds, R., & Zaneveld, J. R. (2014). Chronic nutrient enrichment increases prevalence and severity of coral disease and bleaching. *Global Change Biology*, 20(2), 544–554. <https://doi.org/10.1111/gcb.12450>
- Vermeij, M. J. A., Sandin, S. A., & Samhuri, J. F. (2007). Local habitat distribution determines the relative frequency and interbreeding potential for two Caribbean coral morphospecies. *Evolutionary Ecology*, 21(1), 27–47. <https://doi.org/10.1007/s10682-006-9122-z>
- Wallace, C. C. (1985). Reproduction, recruitment and fragmentation in nine sympatric species of the coral genus *Acropora*. *Marine Biology*, 88(3), 217–233. <https://doi.org/10.1007/BF00392585>
- Ward, S. (1995). The effect of damage on the growth, reproduction and storage of lipids in the scleractinian coral *Pocillopora damicornis* (Linnaeus). *Journal of Experimental Marine Biology and Ecology*, 187(2), 193–206. [https://doi.org/10.1016/0022-0981\(94\)00180-L](https://doi.org/10.1016/0022-0981(94)00180-L)
- Wittenberg, M., & Hunte, W. (1992). Effects of eutrophication and sedimentation on juvenile corals. *Marine Biology*, 112(1), 131–138. <https://doi.org/10.1007/BF00349736>
- Zakai, D., Levy, O., & Chadwick-Furman, N. E. (2000). Experimental fragmentation reduces sexual reproductive output by the reef-building coral *Pocillopora damicornis*. *Coral Reefs*, 19(2), 185–188. <https://doi.org/10.1007/s003380000091>
- Zedler, J. B. (2000). Progress in wetland restoration ecology, 15(10), 402–407. [https://doi.org/10.1016/S0169-5347\(00\)01959-5](https://doi.org/10.1016/S0169-5347(00)01959-5)
- Zeller, D., Booth, S., Davis, G., & Pauly, D. (2007). Re-estimation of small-scale fishery catches for U.S. flag-associated island areas in the western Pacific: The last 50 years. *Fishery Bulletin*, 105(2), 266–277.
- Zhang, B., & Horvath, S. (2005). A general framework for weighted gene co-expression network analysis. *Statistical Applications in Genetics and Molecular Biology*, 4(1). <https://doi.org/10.2202/1544-6115.1128>
- Zhang, Y., Chen, Q., Xie, J. Y., Yeung, Y. H., Xiao, B., Liao, B., ... Qiu, J.-W. (2019). Development of a transcriptomic database for 14 species of scleractinian corals. *BMC Genomics*, 20(1), 1–9.

<https://doi.org/10.1186/s12864-019-5744-8>

10. Supplementary Figures



Supplemental Figure 1: Proportion of Symbiodinium Clade by source *Porites lobata* colony. Proportion of Symbiodinium clades based on highly unique reads (mapping quality > 40) mapping to Clade's genome.



Supplemental Figure 2: Maximum Likelihood tree of phylogenetic relatedness based on cytochrome b (mt-20)

Supplemental Table 1: The number of raw reads, after quality trim, paired and aligned against reference transcriptome.

Sample	Raw	After Q>20	Paired/Alignment rate first ref
1t1_S1_R1_001.fastq.gz	40411887	40262269	
1t1_S1_R2_001.fastq.gz	40411887	40262269	
1t2_S4_R1_001.fastq.gz	29774025	29699824	
1t2_S4_R2_001.fastq.gz	29774025	29699824	
1t4_S7_R1_001.fastq.gz	32014830	31864908	93%
1t4_S7_R2_001.fastq.gz	32014830	31864908	
1t5_S10_R1_001.fastq.gz	37100965	36300314	100/92.98
1t5_S10_R2_001.fastq.gz	37100965	36300314	
1t6_S13_R1_001.fastq.gz	37922178	37600580	100/97.25
1t6_S13_R2_001.fastq.gz	37922178	37600580	
2t1_S2_R1_001.fastq.gz	30286530	30202343	100/95.44

2t1_S2_R2_001.fastq.gz	30286530	30202343	
2t2_S5_R1_001.fastq.gz	31570608	31489229	100/97.58
2t2_S5_R2_001.fastq.gz	31570608	31489229	
2t4_S8_R1_001.fastq.gz	33427925	33304499	100/95.86
2t4_S8_R2_001.fastq.gz	33427925	33304499	
2t5_S11_R1_001.fastq.gz	35788659	34618172	100/94.38
2t5_S11_R2_001.fastq.gz	35788659	34618172	
2t6_S14_R1_001.fastq.gz	45892227	45426834	100/96.94
2t6_S14_R2_001.fastq.gz	45892227	45426834	
3t1_S3_R1_001.fastq.gz	35610993	35469639	100/93.29
3t1_S3_R2_001.fastq.gz	35610993	35469639	
3t2_S6_R1_001.fastq.gz	35848204	35708680	100/94.14
3t2_S6_R2_001.fastq.gz	35848204	35708680	
3t4_S9_R1_001.fastq.gz	31596203	31360005	100/93.1
3t4_S9_R2_001.fastq.gz	31596203	31360005	
3t5_S12_R1_001.fastq.gz	44277047	43809930	100/95.65
3t5_S12_R2_001.fastq.gz	44277047	43809930	
3t6_S15_R1_001.fastq.gz	38370519	38199360	100/96.06
3t6_S15_R2_001.fastq.gz	38370519	38199360	
4t1_S15_R1_001.fastq.gz	44557694	44149932	100/96.79
4t1_S15_R2_001.fastq.gz	44557694	44149932	
4t2_S2_R1_001.fastq.gz	44324757	43865923	100/95/05
4t2_S2_R2_001.fastq.gz	44324757	43865923	
4t4_S11_R1_001.fastq.gz	22963920	22823537	100/97.44
4t4_S11_R2_001.fastq.gz	22963920	22823537	
4t5_S14_R1_001.fastq.gz	39098341	37387406	100/95.25
4t5_S14_R2_001.fastq.gz	39098341	37387406	
4t6_S5_R1_001.fastq.gz	51021407	50820124	100/95.65
4t6_S5_R2_001.fastq.gz	51021407	50820124	

5t1_S1_R1_001.fastq.gz	20530864	20319138	100/78.42
5t1_S1_R2_001.fastq.gz	20530864	20319138	
5t2_S9_R1_001.fastq.gz	6948235	6791713	100/95.57
5t2_S9_R2_001.fastq.gz	6948235	6791713	
5t4_S12_R1_001.fastq.gz	26205810	25566136	100/89.02
5t4_S12_R2_001.fastq.gz	26205810	25566136	
5t5_S3_R1_001.fastq.gz	29358571	29265742	100/95.72
5t5_S3_R2_001.fastq.gz	29358571	29265742	
5t6_S7_R1_001.fastq.gz	21015779	20917704	100/94.75
5t6_S7_R2_001.fastq.gz	21015779	20917704	
6t1_S6_R1_001.fastq.gz	32220307	31856476	100/92.7
6t1_S6_R2_001.fastq.gz	32220307	31856476	
6t2_S10_R1_001.fastq.gz	45404846	44519689	100/89.09
6t2_S10_R2_001.fastq.gz	45404846	44519689	
6t4_S13_R1_001.fastq.gz	42293636	42093497	100/97.36
6t4_S13_R2_001.fastq.gz	42293636	42093497	
6t5_S4_R1_001.fastq.gz	35056090	34734875	100/95.94
6t5_S4_R2_001.fastq.gz	35056090	34734875	
6t6_S8_R1_001.fastq.gz	56476217	56201663	100/94.04
6t6_S8_R2_001.fastq.gz	56476217	56201663	
Average	35,245,642.47	34,887,671.4	
Total	2,114,738,548	2,093,260,282	

Supplemental Table 2: Number of sequences in the reference transcriptome after each filtering step

Raw reference	rRNAfilter	longORFS	Open reading frames	Alien index	Coral Annotated (transcripts/genes)	Symbiodinium Annotated (transcripts/gene)
1963624	1953661	811292	394555	349605	196681/55823	60475/37404

Supplemental Table 3: Benchmarking Universal Single-Copy Orthologs (BUSCO) table of transcriptome completeness scores based on metazoan lineage.

BUSCO Notation	Coral transcriptome	Symbiont transcriptome
Complete Single-copy	194 / 20.34%	38 / 22.22%
Complete Duplicated	694 / 72.75%	4 / 2.34%
Fragmented	21 / 2.2%	53 / 30.99%
Missing	45 / 4.72%	76 / 44.44%
Total represented	93.1%	24.6%

Supplemental Table 4: Table of significantly differentially expressed genes of interest. List of pairwise comparisons, gene categories, gene names, log₂-fold change, uniprot IDs, and significance level of significantly differentially expressed genes which have been previously identified as important in development or stress response. * and ** indicate 0.05 and 0.001 False Discovery Rate (FDR), respectively.

Gene Category	Secondary Category	Comparison	Gene name	Uniprot ID	Log ₂ FC	Significance
Oxidative stress	Heat shock	1V2	97 kDa heat shock protein	A0A2B4SKN4_STYPI	2.023	**
		1V2	Heat shock cognate 71 kDa protein	A0A2B4S326_STYPI	1.639	**
		2V3	97 kDa heat shock protein	A0A2B4SKN4_STYPI	-1.245	*
		1V2	10 kDa heat shock protein, mitochondrial (Chaperonin 10)	A7RHS8_NEMVE	1.539	**
		1V2	Heat shock 70 kDa protein 12A	A0A2B4RHP1_STYPI	-0.837	*
		1V2	Heat shock protein HSP 90-alpha 1	A0A2B4RG70_STYPI	1.012	*
		1V2	Activator of 90 kDa heat shock protein ATPase-like 1	A0A2B4SBB5_STYPI	0.921	*
		1V2	DnaJ homolog subfamily C member 10 (DnaJ homolog subfamily C member 16)	A0A3M6UA46_9CNID	0.672	*
		1V2	DnaJ-like subfamily C member 8	A0A2B4SZE5_STYPI	0.736	*
		1V2	DnaJ-like subfamily C member 3	A0A2B4SDC0_STYPI	2.514	*
		1V2	DnaJ-like subfamily A member 2	A0A2B4SBS3_STYPI	1.073	**
		4V5	DnaJ-like subfamily A member 3, mitochondrial	A0A2B4RSU7_STYPI	0.710	*
		4V5	DnaJ protein-like 1 (Hsp40)	A0A2B4RDU7_STYPI	1.488	*
		1V2	HSP70-1	D1FX74_CHIFL	2.950	**

Oxidative stress	Antioxidant					
		1V2	Thioredoxin	A0A2B4SMK3_STYPI	1.549	*
		1V2	Thioredoxin-like_fold domain-containing protein	A0A3M6UVZ5_9CNID	0.797	*
		1V2	Thioredoxin, mitochondrial	A0A2B4S014_STYPI	0.727	*
		1V2	Peroxiredoxin-1	A0A2B4S129_STYPI	1.222	*
		1V2	Peroxisome proliferator-activated receptor gamma coactivator-related protein 1	A0A2B4RJ99_STYPI	1.511	**
		1V2	Ferritin (EC 1.16.3.1)	A0A2B4SBC3_STYPI	1.253	*
		1V2	Glutathione transferase (EC 2.5.1.18)	A0A2B4SHD3_STYPI	1.359	**
		1V2	Glutathione S-transferase 1	A0A2B4RJ40_STYPI	0.917	*
		1V2	Hypoxia up-regulated protein 1	A0A2B4SVS9_STYPI	1.546	*
		1V5	Hypoxia up-regulated protein 1	A0A2B4SVS9_STYPI	2.068	**
		1V2	Peptide-methionine (S)-S-oxide reductase (EC 1.8.4.11)	A0A3M6U6Z7_9CNID	1.126	*
		1V2	Peptide-methionine (S)-S-oxide reductase (EC 1.8.4.11)	A0A3M6U6Z7_9CNID	1.806	**
		4V5	Ferredoxin--NADP(+) reductase (EC 1.18.1.6) (NADPH:adrenodoxin oxidoreductase, mitochondrial)	A0A2B4SR94_STYPI	-2.051	*
Protein	Degradation	1V2	RING-type E3 ubiquitin transferase (EC 2.3.2.27)	A0A2B4RLS5_STYPI	1.153	**
		1V2	Ubiquitin-conjugating enzyme E2 L3	A0A2B4RQY2_STYPI	1.233	**
		1V2	PRP19/PSO4 homolog (EC 2.3.2.27) (Pre-mRNA-processing factor 19) (RING-type E3 ubiquitin transferase PRP19)	A0A3M6UJC2_9CNID	0.914	**
		1V2	Ubiquitin conjugation factor E4 A	A0A2B4RSY9_STYPI	0.928	**
		1V2	Ubiquitin-fold modifier-conjugating enzyme 1	A0A2B4STM1_STYPI	1.123	**
		1V2	Ubiquitin-like domain-containing protein	A0A3M6UAD0_9CNID	1.123	*
		1V2	E3 ubiquitin-protein ligase HERC2	A0A2B4SA56_STYPI	-1.857	*
		1V2	RBR-type E3 ubiquitin transferase (EC 2.3.2.31)	A0A2B4SUB4_STYPI	1.182	*
		1V2	Ubiquitin-like domain-containing protein	A0A3M6UEK6_9CNID	0.770	*
		1V2	HECT-type E3 ubiquitin transferase (EC 2.3.2.26)	A0A2B4RK80_STYPI	0.825	*
		1V2	Ubiquitin-conjugating enzyme E2 variant 2	T2MCQ1_HYDVU	0.806	*
		1V2	E3 ubiquitin-protein ligase TRIM71	A0A2B4SE87_STYPI	0.816	*
		1V2	E3 ubiquitin-protein ligase (EC 2.3.2.26)	A0A2B4SI89_STYPI	0.726	*

1V2	Ubiquitin carboxyl-terminal hydrolase CYLD	A0A2B4RVQ6_STYPI	-1.405	*
1V2	E3 ubiquitin protein ligase (EC 2.3.2.27)	A0A2B4RWL9_STYPI	0.650	*
1V2	Ubiquitin carboxyl-terminal hydrolase 7 (EC 3.4.19.12) (Ubiquitin thioesterase 7) (Ubiquitin-specific-processing protease 7)	A0A2B4S940_STYPI	0.800	*
1V2	HECT-type E3 ubiquitin transferase (EC 2.3.2.26)	A0A3M6TI31_9CNID	0.654	*
1V2	E3 ubiquitin-protein ligase DTX3L	A0A2B4S0G1_STYPI	-1.036	*
1V2	Ubiquitin	A0A2B4SVQ7_STYPI	-0.965	*
1V2	E3 ubiquitin-protein ligase ZSWIM2	A0A2B4SEP7_STYPI	-0.691	*
1V2	E3 ubiquitin-protein ligase ZNRF2	A0A2B4STQ2_STYPI	0.649	*
1V2	Ubiquitin-conjugating enzyme E2 K	A0A2B4T0N3_STYPI	-1.569	*
1V2	26S proteasome non-ATPase regulatory subunit 6 (26S proteasome regulatory subunit RPN7)	A0A3M6V3Z3_9CNID	1.271	*
1V2	26S proteasome regulatory subunit 7 (Proteasome 26S subunit ATPase 2)	A0A3M6UBT2_9CNID	0.779	*
2V3	E3 ubiquitin-protein ligase TRIM71	A0A2B4SE87_STYPI	-0.976	*
4V5	Ubiquitin carboxyl-terminal hydrolase MINDY (EC 3.4.19.12)	A0A2B4RUW9_STYPI	0.855	*
4V5	E3 ubiquitin-protein ligase RNF213	A0A2B4SMR7_STYPI	-0.977	*
4V5	Ubiquitin-conjugating enzyme E2 variant 2	T2MCQ1_HYDVU	0.802	*
4V5	Ubiquitin-conjugating enzyme E2 L3	A0A2B4RQY2_STYPI	0.916	*
4V5	Ubiquitin-like protein ATG12	A0A3M6TTA0_9CNID	0.782	*
4V5	E3 ubiquitin-protein ligase DTX3L	A0A2B4S0G1_STYPI	-1.162	*
4V5	Ubiquitin carboxyl-terminal hydrolase (EC 3.4.19.12)	A0A3M6TW59_9CNID	0.701	*
4V5	E3 ubiquitin-protein ligase RNF213	A0A2B4SK29_STYPI	-0.990	*
4V5	E3 ubiquitin-protein ligase (EC 2.3.2.27)	A0A3M6TW29_9CNID	-1.418	*
4V5	RBR-type E3 ubiquitin transferase (EC 2.3.2.31)	A0A2B4SUB4_STYPI	1.028	*
4V5	E3 ubiquitin-protein ligase RNF181	A0A2B4RM06_STYPI	2.382	*
4V5	Ubiquitin-like domain-containing protein	A0A3M6V0U6_9CNID	0.934	*

Protein	Synthesis					
		1V2	Protein disulfide-isomerase TMX3	A0A2B4SUK4_STYPI	0.792	*
		1V2	Protein disulfide-isomerase (EC 5.3.4.1)	A0A2B4RL32_STYPI	1.085	*
		1V2	Protein disulfide-isomerase (EC 5.3.4.1)	A0A2B4RVE6_STYPI	-1.885	*
		1V2	Protein disulfide-isomerase (EC 5.3.4.1)	A0A2B4RUX0_STYPI	1.923	*
		1V2	5-aminolevulinate synthase (EC 2.3.1.37) (5- aminolevulinic acid synthase) (Delta-ALA synthase) (Delta- aminolevulinate synthase)	A0A3M6V3W3_9CNID	2.073	**
		1V2	D-aminoacyl-tRNA deacylase (EC 3.1.1.96)	A0A3M6UHT7_9CNID	1.798	**
		1V2	Lysine--tRNA ligase (EC 6.1.1.6) (Lysyl-tRNA synthetase)	A0A3M6TG26_9CNID	1.419	**
		1V2	Glutamyl-tRNA synthetase (EC 6.1.1.15) (EC 6.1.1.17) (Prolyl- tRNA synthetase)	A0A2B4RQE5_STYPI	1.035	**
		1V2	Threonyl-tRNA synthetase (EC 6.1.1.3)	A0A2B4S3J9_STYPI	1.017	**
		1V2	Leucyl-tRNA synthetase (EC 6.1.1.4) (Fragment)	T2M4D5_HYDVU	1.087	**
		1V2	Tryptophanyl-tRNA synthetase (EC 6.1.1.2) (Fragment)	A0A3M6UUJ9_9CNID	0.946	*
		1V2	Arginyl-tRNA synthetase (EC 6.1.1.19)	A0A3M6TU20_9CNID	0.868	*
		1V2	Alanine--tRNA ligase (EC 6.1.1.7)	A7SHU9_NEMVE	1.106	*
		1V2	Tyrosine--tRNA ligase, cytoplasmic (EC 6.1.1.1) (Tyrosyl-tRNA synthetase)	A0A2B4SXR4_STYPI	0.823	*
		1V2	Asparagine--tRNA ligase (EC 6.1.1.22) (Fragment)	T2MI28_HYDVU	0.815	*
		1V2	Aminoacyl-tRNA hydrolase (EC 3.1.1.29)	A0A3M6U0G4_9CNID	1.091	*
		1V2	Seryl-tRNA synthetase (EC 6.1.1.11)	A0A3M6UPT9_9CNID	0.888	*
		1V2	Glutaminyl-tRNA synthetase	A0A2B4RHS6_STYPI	1.112	*
		1V2	Cytoplasmic tRNA 2-thiolation protein 2	A0A3M6UGL7_9CNID	0.822	*
		1V2	Aspartate--tRNA ligase, cytoplasmic (EC 6.1.1.12) (Aspartyl-tRNA synthetase)	A0A3M6TLW8_9CNID	0.743	*
		2V3	Elongation factor Tu	A0A3M6TB99_9CNID	-0.886	*
		4V5	Aspartate aminotransferase (EC 2.6.1.1)	A0A3M6UMV2_9CNID	0.999	**
		4V5	Branched-chain-amino-acid aminotransferase-like protein 2	A0A2B4SFE9_STYPI	1.265	*
		4V5	5-aminoimidazole-4- carboxamide ribonucleotide formyltransferase (EC 2.1.2.3)	A0A2B4SE86_STYPI	0.751	*

			(EC 3.5.4.10) (AICAR transformylase) (AICAR transformylase/inosine monophosphate cyclohydrolase) (Bifunctional purine biosynthesis protein ATIC) (IMP synthase) (Inosinicase) (Phosphoribosylaminoimidazolecarboxamide formyltransferase)		
		4V5	Aminotran_1_2 domain-containing protein	A0A3M6THP0_9CNID	0.661 *
		4V5	Tyrosine aminotransferase (TAT) (EC 2.6.1.5)	A0A3M6U7B9_9CNID	-0.951 *
		4V5	Aminotran_1_2 domain-containing protein	A0A3M6THP4_9CNID	0.629 *
		4V5	Ribosome production factor 2 homolog (Ribosome biogenesis protein RPF2 homolog)	A0A3M6TEH0_9CNID	0.853 *
		4V5	Ribosomal protein S6 kinase (EC 2.7.11.1)	A0A3M6UDF5_9CNID	0.996 *
		4V5	Ribosomal RNA small subunit methyltransferase NEP1	A0A2B4SHV4_STYPI	0.715 *
		4V5	D-aminoacyl-tRNA deacylase (EC 3.1.1.96)	A0A3M6UHT7_9CNID	0.958 *
		4V5	Cytoplasmic tRNA 2-thiolation protein 2	A0A3M6UGL7_9CNID	0.819 *
		4V5	Tryptophanyl-tRNA synthetase (EC 6.1.1.2) (Fragment)	A0A3M6UUJ9_9CNID	0.700 *
		4V5	Aspartate--tRNA ligase, cytoplasmic (EC 6.1.1.12) (Aspartyl-tRNA synthetase)	A0A3M6TLW8_9CNID	0.687 *
		4V5	Lysine--tRNA ligase (EC 6.1.1.6) (Lysyl-tRNA synthetase)	A0A3M6TG26_9CNID	0.840 *
Protein	Transport	1V2	B(0,+)-type amino acid transporter 1	A0A2B4RS97_STYPI	1.175 *
		1V2	Putative sodium-coupled neutral amino acid transporter 10	A0A2B4RSJ0_STYPI	0.839 *
		1V2	High affinity cationic amino acid transporter 1	A0A2B4SC16_STYPI	1.016 **
		4V5	60S ribosomal export protein NMD3 (Fragment)	A7SR71_NEMVE	0.769 *
Protein	Translation initiation	1V2	Eukaryotic translation initiation factor 3 subunit D (eIF3d) (Eukaryotic translation initiation factor 3 subunit 7)	A0A3M6T603_9CNID	1.476 **
		1V2	Eukaryotic translation initiation factor 3 subunit C (eIF3c) (Eukaryotic translation initiation factor 3 subunit 8)	A0A2B4RS17_STYPI	1.246 **
		1V2	Eukaryotic translation initiation factor 3 subunit B (eIF3b)	A0A2B4SKJ2_STYPI	1.227 **

		(Eukaryotic translation initiation factor 3 subunit 9)				
1V2		Eukaryotic translation initiation factor 4E	A0A2B4S6J0_STYPI	1.263	**	
1V2		Eukaryotic translation initiation factor 3 subunit F	A0A2B4SKE2_STYPI	1.423	**	
1V2		Eukaryotic translation initiation factor 3 subunit F (eIF3f) (Eukaryotic translation initiation factor 3 subunit 5)	A7SIV6_NEMVE	1.163	**	
1V2		Eukaryotic translation initiation factor 3 subunit L (eIF3L)	A0A2B4RG74_STYPI	0.985	**	
1V2		Eukaryotic translation initiation factor 3 subunit I (eIF3i)	A0A3M6UR37_9CNID	0.944	**	
1V2		Eukaryotic translation initiation factor 6 (eIF-6)	A0A2B4SAD2_STYPI	0.803	*	
1V2		Eukaryotic translation initiation factor 3 subunit G (eIF3g) (Eukaryotic translation initiation factor 3 RNA-binding subunit) (eIF-3 RNA-binding subunit) (Eukaryotic translation initiation factor 3 subunit 4)	A0A2B4SEK6_STYPI	0.943	*	
1V2		Eukaryotic translation initiation factor 4 gamma 2	A0A2B4S5I7_STYPI	0.776	*	
1V2		Eukaryotic translation initiation factor 4B	A0A2B4RI97_STYPI	0.809	*	
1V2		General transcription factor TFIIB (Transcription initiation factor IIB)	A0A2B4SLJ9_STYPI	0.694	*	
1V2		Eukaryotic translation initiation factor 2 subunit 2	A0A2B4S0K0_STYPI	0.754	*	
1V2		Eukaryotic translation initiation factor 3 subunit E (eIF3e) (Eukaryotic translation initiation factor 3 subunit 6)	A0A2B4RUN6_STYPI	0.680	*	
1V2		Transcription initiation factor TFIID subunit 10	A0A2B4RQR4_STYPI	0.742	*	
1V2		Eukaryotic translation initiation factor 2D (Ligatin)	A0A3M6TFL1_9CNID	0.814	*	
Apoptosis		1V2	Programmed cell death protein 6	A0A2B4RNN3_STYPI	0.649	*
		1V2	Caspase-3	A0A2B4SWS7_STYPI	0.620	*
		1V2	Apoptosis regulator BAX	A0A2B4SFI9_STYPI	1.081	*
		1V2	Bifunctional apoptosis regulator	A0A2B4SJG8_STYPI	0.849	*
		4V5	Caspase-3	A0A2B4SWS7_STYPI	0.775	*
		4V5	Caspase-7	A0A2B4S7Z0_STYPI	1.025	*
		4V5	Programmed cell death protein 6	A0A2B4RNN3_STYPI	1.048	**
		4V5	Apoptosis regulator BAX	A0A2B4SFI9_STYPI	0.837	*
Cell cycle	Growth factor	1V2	Epidermal growth factor-like protein 6	A0A2B4RCT4_STYPI	-1.172	*

	1V2	Fibroblast growth factor (FGF)	A0A3M6TGC7_9CNID	-0.793	*
	1V2	Fibroblast growth factor receptor 1	A0A2B4RSX6_STYPI	-1.185	*
	1V2	Transforming growth factor 3 protein	A0A0A8K7M1_ACRDI	-0.851	*
	2V3	Thyrotroph embryonic factor	A0A2B4S9Y9_STYPI	2.630	**
	2V3	Prokineticin receptor 1	A0A2B4RTA0_STYPI	1.177	*
	2V3	Tyrosine-protein kinase transmembrane receptor ROR2	A0A2B4T378_STYPI	1.988	*
	2V3	Fibroblast growth factor receptor 1-A	A0A2B4RFB7_STYPI	2.407	**
Cytoskeleton	1V2	Beta-actin	J7FRQ2_FIMAN	-1.433	*
	1V2	Tubulin alpha chain (Fragment)	Q2F6H7_ANTEL	0.836	*
	1V2	Tubulin alpha-1C chain	A0A2B4RTB1_STYPI	0.839	*
	1V2	Alpha-tubulin (Fragment)	Q58HH3_HYDEC	1.093	*
	1V2	Tau-tubulin kinase 1	A0A2B4RJC1_STYPI	0.750	*
	1V2	Carbonic anhydrase (EC 4.2.1.1)	A0A3M6U8M2_9CNID	-1.732	**
	1V2	Carbonic anhydrase (EC 4.2.1.1)	A0A2B4S8W1_STYPI	-1.798	*
	1V2	Integrin alpha-V	A0A2B4RUW4_STYPI	1.171	*
	2V3	SWI/SNF-related matrix-associated actin-dependent regulator of chromatin subfamily A member 5	A0A2B4SUJ3_STYPI	-0.842	*
	2V3	Fibrillar collagen (Fragment)	A1XVT2_HYDVU	-2.979	*
	2V3	Matrilin-3	A0A2B4SV97_STYPI	-1.514	*
	2V3	Procollagen-lysine 5-dioxygenase (EC 1.14.11.4)	A0A3M6T4Z7_9CNID	-0.774	*
	2V3	Coactosin-like protein	A0A2B4SSA2_STYPI	-1.891	*
	2V3	Procollagen-lysine 5-dioxygenase (EC 1.14.11.4)	A0A3M6T4Z7_9CNID	-0.774	*
	4V5	Tubulin alpha chain (Fragment)	Q2F6H7_ANTEL	0.755	*
	4V5	Microtubule-actin cross-linking factor 1, isoforms 1/2/3/5	A0A2B4SNH0_STYPI	-0.640	*
DNA damage	4V5	DNA repair protein	A0A2B4SLG3_STYPI	1.197	**
	4V5	DNA repair protein RAD51 homolog	A0A2B4SA40_STYPI	1.278	*
	2V3	DNA mismatch repair protein Msh2	A0A6C0WVN4_ACTEQ	2.276	*
	1V2	DNA topoisomerase I (EC 5.6.2.1) (DNA topoisomerase 1)	A0A2B4SBR9_STYPI	1.163	**
	1V2	DNA topoisomerase (EC 5.6.2.1)	A0A3M6V2M7_9CNID	1.532	**
	1V2	DNA double-strand break repair Rad50 ATPase	A0A2B4RUN1_STYPI	-1.062	*
Calcium	1V2	Calcium-transporting ATPase (EC 7.2.2.10)	A0A3M6T8X3_9CNID	1.517	**

		1V2	Voltage-dependent L-type calcium channel subunit alpha	O97017_STYPI	0.789	*
		1V2	Tyrosine-protein kinase receptor (EC 2.7.10.1)	A0A2B4RSI1_STYPI	0.808	*
		1V2	Calumenin-B	A0A2B4T2P6_STYPI	1.611	*
		1V2	Calreticulin	A0A346HHC6_9CNID	2.311	*
		1V2	Calmodulin	A0A2B4SCT2_STYPI	1.489	*
		2V3	Calmodulin	A0A2B4SCT2_STYPI	-1.396	*
Calcium	Phosphatidylinositol signaling	1V2	Phosphatidylinositol transfer protein beta isoform	A0A2B4SGX6_STYPI	1.276	**
		1V2	Phosphatidylinositol 3,4,5-trisphosphate 3-phosphatase TPTE2	A0A2B4SN32_STYPI	1.612	**
		1V2	Phosphatidylinositol-4,5-bisphosphate 4-phosphatase (EC 3.1.3.78)	A0A2B4S1C9_STYPI	0.808	*
		1V2	Phosphatidylinositol-binding clathrin assembly protein	A0A2B4T1I6_STYPI	0.768	*
		1V2	D-inositol 3-phosphate glycosyltransferase	A0A2B4RXX4_STYPI	0.778	*
		1V2	Diphosphoinositol polyphosphate phosphohydrolase 1	A0A2B4SXX6_STYPI	0.894	*
		1V2	Phosphatidylinositol 4-kinase type 2 (EC 2.7.1.67)	A0A2B4RZ42_STYPI	0.724	*
		1V2		A0A2B4RNA5_STYPI	0.687	*
		1V2	Phosphatidylinositol-3-phosphate phosphatase (EC 3.1.3.48) (EC 3.1.3.64)	A0A3M6TG06_9CNID	0.655	*
		1V2	Phosphoinositide phospholipase C (EC 3.1.4.11)	A0A2B4RY04_STYPI	2.100	*
		1V2	Peroxisome proliferator-activated receptor gamma coactivator-related protein 1	A0A2B4RJR9_STYPI	1.511	**
		1V2	Serine/threonine-protein kinase receptor (EC 2.7.11.30)	A0A2B4SU78_STYPI	0.894	*
Lipid metabolism		1V2	Acyl-coenzyme A thioesterase THEM4	A0A2B4STD7_STYPI	1.448	**
		1V2	O-acyltransferase	A7RML0_NEMVE	-1.721	*
		4V5	Lipid droplet-associated hydrolase (Lipid droplet-associated serine hydrolase)	A0A3M6U228_9CNID	0.938	**
		4V5	Elongation of very long chain fatty acids protein (EC 2.3.1.199) (Very-long-chain 3-oxoacyl-CoA synthase)	A0A3M6U3H4_9CNID	1.456	**
		4V5	Sphingolipid 4-desaturase (EC 1.14.19.17)	A0A3M6TES2_9CNID	1.163	**
		4V5	3-hydroxyacyl-CoA dehydrogenase type-2	A0A2B4SYP0_STYPI	0.930	*

Carbohydrate metabolism	Glycolysis	1V2	Phosphoglycerate mutase (EC 5.4.2.12) (2,3-diphosphoglycerate-independent)	A0A2B4RLF3_STYPI	1.934	**
		2V3	Phosphoglycerate mutase (2,3-diphosphoglycerate-independent) (EC 5.4.2.12)	A0A2B4RLF3_STYPI	-1.122	*
Carbohydrate metabolism	Citric acid cycle	1V2	Aconitate hydratase, mitochondrial (Aconitase) (EC 4.2.1.-)	A0A3M6UMV8_9CNID	1.008	**
		1V2	Mitochondrial pyruvate carrier	A0A3M6TNI8_9CNID	1.111	**
		1V2	Pyruvate dehydrogenase E1 component subunit alpha (EC 1.2.4.1)	A0A3M6UH40_9CNID	0.704	*
		1V2	Dihydrolipoamide acetyltransferase component of pyruvate dehydrogenase complex (EC 2.3.1.-)	A0A2B4SNL5_STYPI	0.763	*
		1V2	Succinate--CoA ligase [GDP-forming] subunit beta, mitochondrial (EC 6.2.1.4) (GTP-specific succinyl-CoA synthetase subunit beta) (G-SCS) (GTPSCS) (Succinyl-CoA synthetase beta-G chain) (SCS-betaG)	A0A3M6V3V3_9CNID	0.664	*
		4V5	Succinate dehydrogenase [ubiquinone] cytochrome b small subunit	A0A3M6V4T9_9CNID	1.093	**
		4V5	Succinate dehydrogenase (quinone) (EC 1.3.5.1) (Fragment)	A7SCJ3_NEMVE	1.142	**
		4V5	Malate dehydrogenase (EC 1.1.1.37)	A0A2B4RQH9_STYPI	0.789	*
		4V5	Mitochondrial pyruvate carrier	A0A3M6UPW1_9CNID	1.618	*
		4V5	Mitochondrial pyruvate carrier	A0A3M6TNI8_9CNID	0.769	*
Cellular transport	Protein transport	1V2	Rab GDP dissociation inhibitor	A0A2B4SJQ6_STYPI	0.874	*
		1V2	Ras-related protein Rab-32A	A0A2B4RQV9_STYPI	-1.317	*
		1V2	Rab-3A-interacting protein	A0A2B4SGR3_STYPI	0.980	*
		1V2	Ras-related protein Rab-36	A0A2B4SF06_STYPI	0.877	*
		1V2	Ras-related protein Rab-2	A0A2B4SQJ0_STYPI	0.783	*
		1V2	Ras-related protein Rab-7L1	A0A2B4SHI3_STYPI	1.020	*
Cellular transport	Proton transport	1V2	Vacuolar proton pump subunit B (V-ATPase subunit B) (Vacuolar proton pump subunit B)	A0A2B4S736_STYPI	1.045	**
		1V2	V-type proton ATPase 21 kDa proteolipid subunit	A0A2B4SQV4_STYPI	0.941	*
		1V2	Proton-translocating NAD(P)(+) transhydrogenase (EC 7.1.1.1)	A0A2B4SX48_STYPI	0.739	*

	1V2	V-type proton ATPase subunit E	A0A2B4SI00_STYPI	0.727	*
	4V5	V-type proton ATPase 21 kDa proteolipid subunit	A0A2B4SQV4_STYPI	0.880	*
	4V5	V-type proton ATPase subunit C	A7RL79_NEMVE	0.656	*
Cellular transport	1V2	Sodium/potassium-transporting ATPase subunit beta-1-interacting protein 1	A0A2B4SDN7_STYPI	0.939	*
	1V2	Transportin-1	A0A2B4SM89_STYPI	1.381	*
	1V2	Magnesium transporter protein 1	A0A2B4T0L4_STYPI	0.860	*
	1V2	Major facilitator superfamily domain-containing protein 5 (Molybdate transporter 2 homolog) (Molybdate-anion transporter) (Fragment)	A7SG46_NEMVE	-0.778	*
	1V2	Copper transporter	A0A2B4S5R8_STYPI	1.685	*
	1V2	Solute carrier organic anion transporter family member	A0A3M6TG97_9CNID	0.997	*
	1V2	Solute carrier organic anion transporter family member	A0A2B4S483_STYPI	0.630	*
	1V2	Phospholipid-transporting ATPase (EC 7.6.2.1)	A0A2B4S7M6_STYPI	0.643	*
	1V2	Glycine betaine transporter OpuD	A0A2B4RX87_STYPI	1.088	*
	1V2	Protein transport protein SEC23	A0A3M6U474_9CNID	0.638	*
	1V2	Putative sodium-coupled neutral amino acid transporter 10	A0A2B4RSJ0_STYPI	0.839	*
	1V2	Solute carrier family 30 member 9 (Zinc transporter 9)	A0A3M6TT97_9CNID	0.775	*
	1V2	Solute carrier family 30 member 9 (Zinc transporter 9)	A0A3M6TT97_9CNID	0.775	*
	1V2	Zinc transporter ZIP11	A0A2B4SI40_STYPI	0.688	*
	1V2	Zinc transporter ZIP13	A0A2B4RI41_STYPI	0.863	*
	1V2	Zinc transporter SLC39A7	A0A2B4RYI4_STYPI	2.294	*
	1V3	Vesicle-fusing ATPase (EC 3.6.4.6)	A7SJ61_NEMVE	1.018	**
	2V3	Monocarboxylate transporter 10	A0A2B4S850_STYPI	-1.079	*
	4V5	Zinc transporter ZIP11	A0A2B4SI40_STYPI	0.734	*
	4V5	Zinc transporter 2	A0A2B4RP90_STYPI	1.189	**
	4V5	Sodium/potassium-transporting ATPase subunit beta-1	A0A2B4SP72_STYPI	1.167	**
	4V5	ABC transporter domain-containing protein (Fragment)	A0A3M6TFU8_9CNID	1.255	*
	4V5	Mitochondrial coenzyme A transporter SLC25A42	A0A2B4RV20_STYPI	0.800	*
	4V5	Sodium/potassium-transporting ATPase subunit alpha (Fragment)	A0A3M6TW19_9CNID	1.038	*

		4V5	Sodium-and chloride-dependent GABA transporter 2	A0A2B4S0L0_STYPI	0.963	*
		4V5	Monocarboxylate transporter 10	A0A2B4RV02_STYPI	0.736	*
		4V5	Sodium-coupled monocarboxylate transporter 1	A0A2B4SZY2_STYPI	0.778	*
RNA/DNA	Transcription	1V2	RNA helicase (EC 3.6.4.13)	T2M5C3_HYDVU	1.629	**
		1V2	RNA helicase (EC 3.6.4.13)	A0A2B4RYD4_STYPI	-1.431	**
		1V2	RNA helicase (EC 3.6.4.13)	A0A3M6TB93_9CNID	2.679	**
		1V2	RNA helicase (EC 3.6.4.13)	A0A3M6UH79_9CNID	1.019	**
		1V2	RNA helicase (EC 3.6.4.13)	A0A3M6TE03_9CNID	1.008	**
		1V2	RNA helicase (EC 3.6.4.13)	J3T9N7_FIMAN	0.935	**
		1V2	RNA helicase (EC 3.6.4.13)	A0A2B4SNV4_STYPI	0.910	**
		1V2	RNA helicase (EC 3.6.4.13)	A0A2B4RCN6_STYPI	-1.190	*
		1V2	RNA helicase (EC 3.6.4.13)	A0A3M6U918_9CNID	1.985	*
		1V2	RNA helicase (EC 3.6.4.13)	A0A2B4R8X2_STYPI	0.981	*
		1V2	RNA helicase (EC 3.6.4.13)	A0A2B4SVS7_STYPI	0.769	*
		1V2	RNA helicase (EC 3.6.4.13)	A0A3M6U6L2_9CNID	-0.774	*
		4V5	RNA helicase (EC 3.6.4.13)	T2MDB0_HYDVU	-1.254	*
		4V5	RNA-directed RNA polymerase (EC 2.7.7.48)	A0A2B4RG40_STYPI	-1.565	*
		4V5	RNA-directed DNA polymerase from mobile element jockey	A0A2B4SBK8_STYPI	-1.086	*
		4V5	RNA-directed DNA polymerase from mobile element jockey	A0A2B4S1E6_STYPI	-1.212	*
		4V5	RNA-directed DNA polymerase from mobile element jockey	A0A2B4T008_STYPI	-1.327	*
		4V5	RNA-directed DNA polymerase (EC 2.7.7.49)	A0A2B4SZG6_STYPI	-0.889	*
RNA/DNA	Synthesis	4V5	AIR carboxylase (EC 4.1.1.21) (EC 6.3.2.6) (Phosphoribosylaminoimidazole carboxylase) (Phosphoribosylaminoimidazole-succinocarboxamide synthase) (SAICAR synthetase)	A0A2B4RQJ5_STYPI	2.521	**
Cellular energy		1V2	Adenylate kinase (EC 2.7.4.3) (ATP-AMP transphosphorylase) (ATP:AMP phosphotransferase) (Adenylate kinase cytosolic and mitochondrial) (Adenylate monophosphate kinase)	A0A3M6TCQ4_9CNID	0.932	**
Cellular energy	ATP generation	1V2	ATP synthase subunit alpha	A0A2B4T1C4_STYPI	1.136	**

		1V2	ATP synthase subunit gamma	A7RNI6_NEMVE	0.890	*
		1V2	ATP synthase F(0) complex subunit B1, mitochondrial	A0A2B4SSQ3_STYPI	1.210	*
		1V2	ATP synthase F(0) complex subunit B1, mitochondrial	A0A2B4SSQ3_STYPI	1.210	*
		1V2	ATP synthase subunit beta (EC 7.1.2.2)	A0A2B4SJB0_STYPI	0.897	*
		4V5	ATP synthase subunit alpha	A0A2B4T1C4_STYPI	0.839	*
Cellular energy	Electron transport chain	1V2	Electron transfer flavoprotein subunit alpha (Alpha-ETF)	A0A3M6U8Q7_9CNID	0.935	*
		1V2	Complex I-9kD (NADH dehydrogenase [ubiquinone] flavoprotein 3, mitochondrial) (NADH-ubiquinone oxidoreductase 9 kDa subunit)	A0A2B4SMJ8_STYPI	0.834	*
		1V2	Complex I-30kD (NADH dehydrogenase [ubiquinone] iron-sulfur protein 3, mitochondrial) (NADH-ubiquinone oxidoreductase 30 kDa subunit)	A0A3M6TYS4_9CNID	0.731	*
		1V2	NADH dehydrogenase [ubiquinone] flavoprotein 2, mitochondrial	A0A2B4SFU3_STYPI	0.697	*
		1V2	Complex I-B14.7 (NADH dehydrogenase [ubiquinone] 1 alpha subcomplex subunit 11) (NADH-ubiquinone oxidoreductase subunit B14.7)	A0A3M6TFB3_9CNID	0.686	*
		1V2	Complex I-19kD (NADH dehydrogenase [ubiquinone] 1 alpha subcomplex subunit 8) (NADH-ubiquinone oxidoreductase 19 kDa subunit)	A0A3M6TW27_9CNID	0.672	*
		1V2	Complex I-ESSS (NADH dehydrogenase [ubiquinone] 1 beta subcomplex subunit 11, mitochondrial) (NADH-ubiquinone oxidoreductase ESSS subunit)	A0A2B4RK25_STYPI	0.706	*
		1V2	NADH dehydrogenase [ubiquinone] flavoprotein 1, mitochondrial (EC 7.1.1.2)	A0A2B4REL4_STYPI	0.693	*
		1V2	NADH dehydrogenase [ubiquinone] 1 alpha subcomplex subunit 9, mitochondrial	A0A2B4T2D6_STYPI	0.701	*
		1V2	Complex I-49kD (NADH-ubiquinone oxidoreductase 49 kDa subunit)	A0A3M6TNT9_9CNID	0.800	*
		1V2	Complex I-49kD (NADH-ubiquinone oxidoreductase 49 kDa subunit)	A0A2B4S4S7_STYPI	0.878	*

1V2	Cytochrome c domain-containing protein	A0A3M6UD76_9CNID	1.462	**
1V2	Cytochrome c oxidase subunit 5B, mitochondrial	A0A2B4RPW9_STYPI	1.383	**
1V2	Cytochrome c oxidase polypeptide VIIc	A0A3M6U6A2_9CNID	2.770	*
1V2	Cytochrome c oxidase subunit (Cytochrome c oxidase polypeptide VIa)	A0A3M6TGK2_9CNID	0.984	*
1V2	Cytochrome c oxidase polypeptide Va (Cytochrome c oxidase subunit 5A, mitochondrial)	A0A2B4RZU5_STYPI	1.172	*
1V2	Cytochrome b(558) alpha chain (Cytochrome b-245 light chain) (Cytochrome b558 subunit alpha) (Neutrophil cytochrome b 22 kDa polypeptide) (Superoxide-generating NADPH oxidase light chain subunit) (p22 phagocyte B-cytochrome) (p22-phox)	A0A3M6TPG0_9CNID	0.984	*
1V2	Cytochrome b-245 heavy chain	A0A2B4REC7_STYPI	1.836	**
1V2	Complex III subunit 8 (Complex III subunit VIII) (Cytochrome b-c1 complex subunit 8) (Ubiquinol-cytochrome c reductase complex 9.5 kDa protein) (Ubiquinol-cytochrome c reductase complex ubiquinone-binding protein QP-C)	A0A3M6UGP1_9CNID	1.361	**
1V2	Cytochrome b-c1 complex subunit 6, mitochondrial	A0A2B4SXR9_STYPI	1.288	*
1V2	Cytochrome b-c1 complex subunit 7	A0A3M6TEI6_9CNID	1.917	*
1V2	Cytochrome b5 heme-binding domain-containing protein	A0A3M6U6V7_9CNID	1.443	*
1V2	Cytochrome b5 heme-binding domain-containing protein (Fragment)	A0A3M6V3E2_9CNID	0.778	*
1V2	Cytochrome b5 heme-binding domain-containing protein	A0A3M6TUM8_9CNID	1.102	*
1V2	Cytochrome P450 4F5	A0A2B4RGC5_STYPI	-0.925	*
1V2	Cytochrome P450 1A1	A0A2B4S3Z7_STYPI	-0.740	*
1V2	NADPH--cytochrome P450 reductase	A0A2B4S487_STYPI	0.755	*
4V5	Complex I-49kD (NADH-ubiquinone oxidoreductase 49 kDa subunit)	A0A2B4S4S7_STYPI	1.503	**
4V5	Electron transfer flavoprotein-ubiquinone oxidoreductase (ETF-QO) (EC 1.5.5.1)	A0A2B4SE12_STYPI	1.547	**

		4V5	Cytochrome b-561 (Cytochrome b561)	A0A3M6UV69_9CNID	1.030	**
Other	Histone	1V2	Histone deacetylase (EC 3.5.1.98)	A0A2B4SH89_STYPI	1.470	**
		1V2	Histone H1-delta	A0A2B4SSY5_STYPI	-1.461	*
		1V2	Histone-binding protein RBBP7	A0A2B4SQP1_STYPI	0.846	*
		1V2	Putative histone-lysine N- methyltransferase PRDM6	A0A2B4SW04_STYPI	2.729	*
		1V2	Histone chaperone asf1	A0A2B4SNY5_STYPI	0.776	*
		1V2	Histone acetyltransferase (EC 2.3.1.48)	A0A3M6TT41_9CNID	1.390	*
		1V2	Histone acetyltransferase (EC 2.3.1.48)	A0A2B4SF80_STYPI	0.682	*
		1V2	[Histone H3]-trimethyl-L- lysine(4) demethylase (EC 1.14.11.67)	A0A3M6UK63_9CNID	0.623	*
Other	Immune response	1V2	Complement C3	A0A2B4SP95_STYPI	-3.003	*
		1V2	Complement C1q and tumor necrosis factor-related protein 9B	A0A2B4SXX5_STYPI	-0.775	*